BJ www.biochemj.org

BJ Signal

Biochem. J. (2008) **415**, 353–365 (Printed in Great Britain) doi:10.1042/BJ20080309

online data

The selectivity of inhibitors of protein kinase CK2: an update

Mario A. PAGANO*†[1], Jenny BAIN‡[1], Zygmunt KAZIMIERCZUK§[2], Stefania SARNO*†, Maria RUZZENE*†, Giovanni DI MAIRA*†, Matthew ELLIOTT‡, Andrzej ORZESZKO||, Giorgio COZZA*, Flavio MEGGIO* and Lorenzo A. PINNA*†[1,2]

*Department of Biological Chemistry and CNR Institute of Neurosciences, University of Padova, viale G. Colombo 3, 35131 Padova, Italy, †Venetian Institute for Molecular Medicine (VIMM), via Orus 2, 35129 Padova, Italy, and ‡Division of Signal Transduction Therapy and Medical Research Council, Protein Phosphorylation Unit, University of Dundee, Dundee DD1 5EH, Scotland, U.K., §Laboratory of Experimental Pharmacology, Polish Academy of Sciences Medical Research Center, 5 Pawinskiego St. 02-106 Warsaw, Poland, and ||Military University of Technology, 2 Kaliskiego Street, 00-908 Warsaw, Poland

CK2 (casein kinase 2) is a very pleiotropic serine/threonine protein kinase whose abnormally high constitutive activity has often been correlated to pathological conditions with special reference to neoplasia. The two most widely used cell permeable CK2 inhibitors, TBB (4,5,6,7-tetrabromo-1*H*-benzotriazole) and DMAT (2-dimethylamino-4,5,6,7-tetrabromo-1*H*-benzimidazole), are marketed as quite specific CK2 blockers. In the present study we show, by using a panel of approx. 80 protein kinases, that DMAT and its parent compound TBI (or TBBz; 4,5,6,7-tetrabromo-1*H*-benzimidazole) are potent inhibitors of several other kinases, with special reference to PIM (provirus integration site for Moloney murine leukaemia virus)1, PIM2, PIM3, PKD1 (protein kinase D1), HIPK2 (homeodomain-interacting protein kinase 2) and DYRK1a (dual-specificity tyrosine-phosphorylated and -regulated kinase 1a). In contrast, TBB is significantly more selective toward CK2, although it also inhibits PIM1 and PIM3. In an attempt to improve selectivity towards CK2 a library of 68 TBB/TBI-related compounds have been tested for their ability to discriminate between CK2, PIM1, HIPK2 and DYRK1a, ending up with seven compounds whose efficacy toward CK2 is markedly higher than that toward the second most inhibited kinase. Two of these, K64 (3,4,5,6,7-pentabromo-1*H*-indazole) and K66 (1-carboxymethyl-2-dimethylamino-4,5,6,7-tetrabromo-benzimidazole), display an overall selectivity much higher than TBB and DMAT when tested on a panel of 80 kinases and display similar efficacy as inducers of apoptosis.

Key words: ATP mimetics, casein kinase 2 (CK2) inhibitor, drug design, homeodomain-interacting protein kinase 2 (HIPK2), provirus integration site for Moloney murine leukaemia virus 1 (PIM1), selectivity.

INTRODUCTION

CK2 (an acronym derived from the misnomer 'casein kinase' 2) denotes one of the most pleiotropic serine/threonine protein kinases, with more than 300 protein substrates already identified [1] and responsible for the generation of a substantial proportion of the eukaryotic phosphoproteome [2]. Such an extreme pleiotropy may, at least partially, account for the observation that CK2 catalytic activity is not controlled by second messengers, phosphorylation events or association of its catalytic (α and/or α') domain with its regulatory β-subunits to give a 'constitutively active' heterotetrameric holoenzyme [3,4]. In turn constitutive activity and lack of physiological down-regulatory devices may underlie the pathogenic potential of CK2, whose abnormally elevated levels have been correlated to a number of global diseases, with special reference to neoplasia. Abnormally high levels of CK2 have been documented in a number of cancers including kidney [5], mammary gland [6], lung [7], head and neck [8] and prostate [9], and a number of experimental models and coincidental arguments support the notion that CK2 promotes cell survival through the regulation of oncogenes and plays a global anti-apoptotic role (reviewed by Duncan and Litchfield [10]).

Studies aimed at dissecting the multifarious functions of CK2 are hampered by its constitutive activity and limitations in strategies exploited to inhibit the cellular activity of other kinases, notably usage of kinase-inactive dominant-negative mutants and RNAi (RNA interference) techniques. These techniques are hindered by long half-life, cellular localization and high expression of endogenous CK2 in cells [10]. Indeed conflicting results regarding the effectiveness of down-regulation devices (e.g. compare Wang et al. [11] with Seeber et al. [12]) have been reported, suggesting that RNAi or antisense strategies sometimes may be inefficient, requiring continual treatment of cells in order to achieve effective CK2 depletion.

These limitations make the pharmacological approach the most promising tool to dissect the cellular functions of CK2 and explain why considerable efforts have been made to develop specific cell-permeable CK2 inhibitors (reviewed in Sarno et al. [13]). Some of these inhibitors have proved to be extremely helpful for the identification of CK2 cellular targets and the implication of CK2 in specific cellular functions, as well as in malignancy and defective apoptosis of cancer cells [10,13,14]. In a few cases the concept that the observed pharmacological effect was actually mediated by CK2 inhibition was validated by transfecting the cells with CK2 mutants refractory to inhibitors [15,16]. Generally, however, the implication of CK2 was inferred from the assumption that the compounds used are 'specific' inhibitors of this kinase. In this respect the most successful commercially available

Abbreviations used: CDK, cyclin-dependent kinase; CK2, casein kinase 2; DMAT, 2-dimethylamino-4,5,6,7-tetrabromo-1*H*-benzimidazole; DRB, 5,6-dichloro-1-β-D-ribofuranosylbenzimidazole; DYRK, dual-specificity tyrosine-phosphorylated and -regulated kinase; ERK, extracellular-signal-regulated kinase; HIPK, homeodomain-interacting protein kinase; MSK, mitogen- and stress-activated protein kinase; MTT, 3-(4,5-dimethylthiazol-2-yl)-3,5-diphenyltriazolium bromide; PKD, protein kinase D; PIM, provirus integration site for Moloney murine leukaemia virus; RNAi, RNA interference; TBB, 4,5,6,7-tetrabromo-1*H*-benzotriazole; TBI (or TBBz), 4,5,6,7-tetrabromo-1*H*-benzimidazole.

[1] These authors contributed equally to the present study.

[2] Correspondence may be addressed to either of these authors (email lorenzo.pinna@unipd.it or zygmunt_kazimierczuk@sggw.pl).

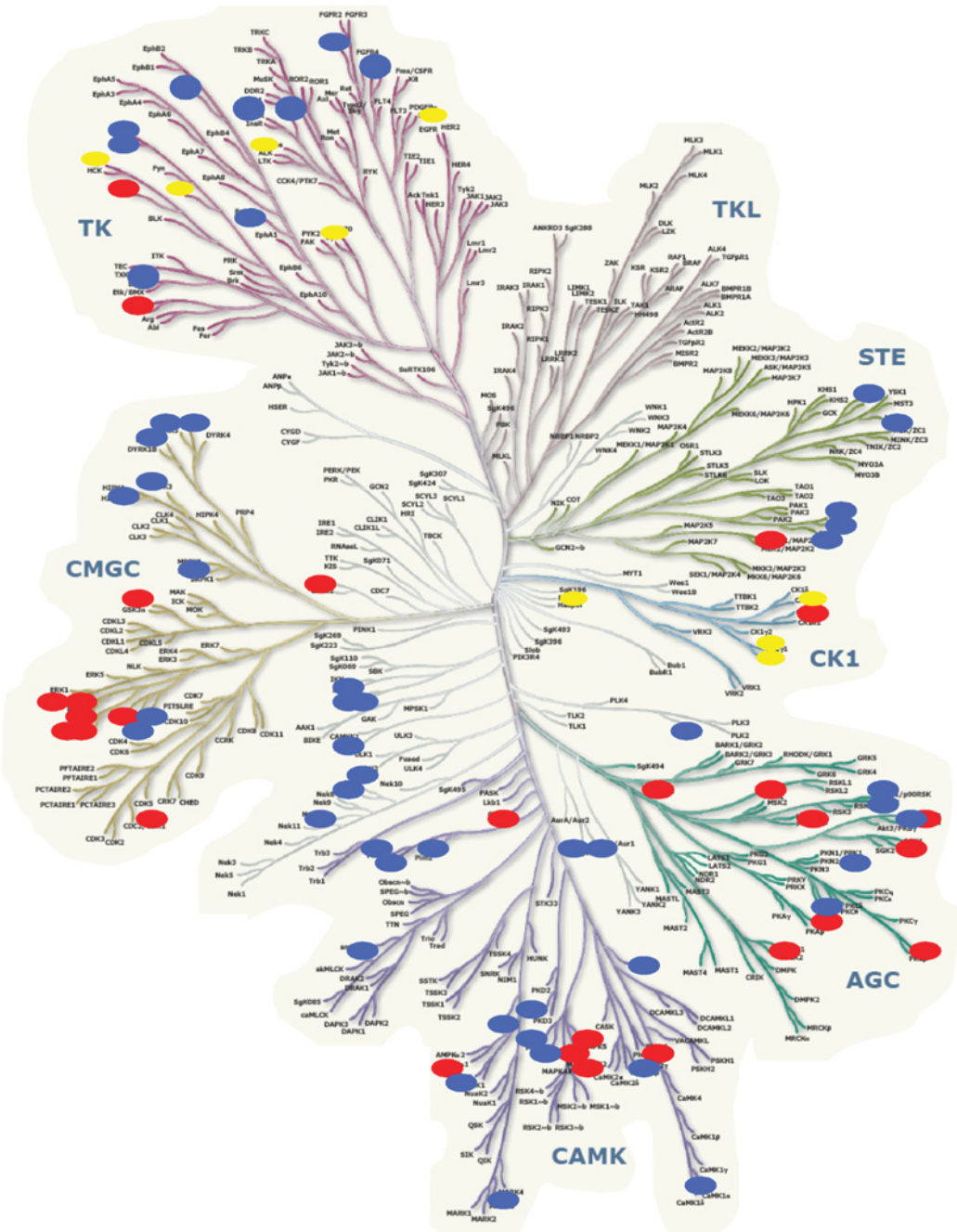

Figure 1 Distribution within the human kinome of protein kinases tested for selectivity against CK2 inhibitors

The human kinome [49] is shown and the protein kinases included in the selectivity profiling tested for selectivity are indicated by blue circles. Protein kinases included in the 2001 TBB selectivity test [18] are marked in red. In yellow are shown the additional protein kinases tested only in Padova under conditions described previously [18]. This is provided courtesy of and with permission from Cell Signaling Technology (www.cellsignal.com).

'specific' CK2 inhibitors are: (i) TBB (4,5,6,7-tetrabromo-1*H*-benzotriazole) also termed TBBt to distinguish it from its analogue TBI (or TBBz; 4,5,6,7-tetrabromo-1*H*-benzimidazole), also a potent inhibitor of CK2 [17], and (ii) DMAT (2-dimethylamino-4,5,6,7-tetrabromo-1*H*-benzimidazole). The specificities of TBB and DMAT, although not that of TBI, have been assessed on a panel of approx. 30 protein kinases, none of which was inhibited as drastically as CK2 [18,19]. In contrast, other commercially available CK2 inhibitors, notably quercetin, apigenin and emodin, did not display a comparable selectivity [20,21]. Recently, however, the panel of protein kinases currently available for running selectivity profiles has been substantially enlarged, to include approx. 80 kinases representative of nearly all of the branches of the kinome (see Figure 1). This has provided a tool for updating the selectivity of kinase inhibitors and has led to the discovery of 'new' targets for 'old' inhibitors [22]. This latter study [22] did not include any CK2 'specific inhibitor'. On the other hand the solution of the crystal structure of the complex between CK2 and TBI/TBBz [23] has allowed a comparison with the structures of the complexes with TBB [24] and with DMAT [25] leading to the conclusion that, despite their structural similarities, TBB binds in a quite different manner than TBI

and DMAT. Taken together these observations prompted us to profile the selectivity of TBB, DMAT and TBI on the new large panel of protein kinases now available. The results reported in the present study support the view that the selectivity of TBB for CK2 is narrower than that of DMAT and TBI/TBBz, which are also powerful inhibitors of kinases belonging to the PIM (provirus integration site for Moloney murine leukaemia virus), HIPK (homeodomain-interacting protein kinase), DYRK (dual-specificity tyrosine-phosphorylated and -regulated kinase) and PKD (protein kinase D) families, and led to the identification of new and more selective inhibitors of CK2.

EXPERIMENTAL

Enzymes

Native CK2 was purified from rat liver [26]. Human recombinant α and β subunits of CK2 were expressed in *Escherichia coli* and the holoenzyme was reconstituted and purified as previously described [27]. Single and double mutants of the CK2α subunit were generated as reported in [19,20]. The source of all of the other protein kinases used for specificity assays are as previously either described or referenced [22].

Cell culture, treatment and viability assay

The human leukaemia Jurkat T-cell line was maintained in RPMI-1640 medium, supplemented with 10% (v/v) foetal calf serum, 2 mM L-glutamine, 100 units/ml penicillin and 100 μg/ml streptomycin. For the treatment, cells were suspended at a density of 10^6 cells/ml in a medium containing 1% (v/v) foetal calf serum, then incubated at 37 °C in the presence of the compounds at the indicated concentrations. Control cells were treated with equal amounts of solvent (0.5% DMSO). At the end of incubations, cells were lysed by the addition of hypo-osmotic buffer, as previously described [20]. Cell viability was assessed by means of MTT [3-(4,5-dimethylthiazol-2-yl)-3,5-diphenyltriazolium bromide] reagent, whereas apoptosis was evaluated by means of the Cell Detection Elisa kit (Roche), based on the quantification of nucleosomes present in the cytosol of the apoptotic cells, following the manufacturer's protocol. For each determination, 10000 cells were used.

Phosphorylation assays

CK2 activity was tested in a final volume of 25 μl containing 50 mM Tris/HCl (pH 7.5), 100 mM NaCl, 12 mM $MgCl_2$, 100 μM synthetic peptide substrate RRRADDSDDDDD and 0.02 mM [γ-^{33}P]ATP (500–1000 c.p.m./pmol), unless otherwise indicated, and incubated for 10 min at 37 °C. Native CK2 purified from rat liver (0.5–1 pmol) was usually the phosphorylating enzyme, unless otherwise indicated. Assays were stopped by the addition of 5 μl of 0.5 M orthophosphoric acid before spotting aliquots on to phosphocellulose filters. Filters were washed in 75 mM phosphoric acid (5–10 ml each) four times, followed by once in methanol and were dried before counting.

PIM1 activity was determined following the same procedure, by incubating the kinase in the presence of 50 mM Tris/HCl (pH 7.5), 0.1% 2-mercaptoethanol, 0.1 mM EGTA, 30 μM synthetic peptide substrate RKRRQTSMTD [29] and 100 μM [γ-^{33}P]ATP. HIPK2 activity was determined under the same conditions used for PIM1 assays, except for ATP which was 20 μM and the use of 10 μg of MBP (myelin basic protein) as phosphorylatable substrate.

Conditions for the activity assays of all other protein kinases tested in selectivity experiments are as described or referenced previously [22].

Kinetic determination

Initial velocities were determined at each of the substrate concentrations tested. K_m values were calculated from Lineweaver–Burk double-reciprocal plots of the data either in the absence or in the presence of increasing concentrations of inhibitor. Inhibition constants were then calculated by linear regression analysis of K_m/V_{max} versus inhibitor concentration plots. Alternatively, inhibition constants were also deduced from the IC_{50}/K_i Cheng–Prusoff relationship [28] by determining the IC_{50} for each compound at a 1 μM ATP concentration, i.e. much below the K_m value. The rationale underlying this approach, based on the assumption that inhibition is competitive with respect to ATP, is illustrated by Burlingham and Widlanski [29].

Molecular modelling

The human CK2α subunit and PIM1 catalytic subunit were retrieved from the PDB (PDB codes 1JWH and 3C4E respectively) and processed in order to remove the ligands and water molecules. Hydrogen atoms were added to the protein structure using standard geometries with the MOE program. To minimize contacts between hydrogens, the structures were subjected to Amber94 force-field minimization until the rms (root mean square) of conjugate gradient was <0.1 kcal $\cdot$ mol^{-1} $\cdot$ Å^{-1} (1 Å = 0.1 nm) keeping the heavy atoms fixed at their crystallographic positions. To strictly validate the model generated and to calibrate the high-throughput docking protocol, a small database of known CK2 and PIM1 inhibitors was built and a set of docking runs was performed. After the calibration phase, flexible ligand-docking steps with three different programs, MOE-Dock, Glide and Gold, were performed essentially as described previously [30].

Synthesis of new analogues

All chemicals and solvents used for the syntheses were purchased from Sigma–Aldrich. Details for the synthesis of most benzimidazoles and benzotriazoles have been described previously [19,25,31,32]. New derivatives discussed in the present paper have been synthesized as described below.

The synthesis of 4,5,6,7-tetrabromo-*1H*-indazole (**1**, K59) was realized by the ring closure of the intermediate 3,4,5,6-tetrabromo-2-methyl-*N*-nitroso-*N*-acetylaniline [33]. The bromination of **1** was performed using bromine in anhydrous acetic acid, at elevated temperature, yielding the pentabromoderivative **4** (K64). Alkylation of **1** with 2-bromoethanol and 2-dimethylaminoethylchloride provided, as expected, two regioisomers each, **2a** and **2b** (K60 and K62) and **3a** and **3b** (K61 and K63) respectively. The mixtures of N^1- and N^2-substituted derivatives were separated by flash chromatography and the structures of the derivatives were determined by comparing their ^{1}H NMR- and UV-spectra with those of the respective known N-substituted indazoles [34,35]. Dissociation constants of **1** (10.6) and **4** (8.40) measured in 50% aqueous ethanol showed the inductive effect of bromine substituents by lowering the respective pK_a value by several units as compared with that of unsubstituted indazole (14.0). A similar effect was observed for TBB ($pKa = 4.95$) and 4,5,6,7-tetrabromobenzimidazole ($pK_a = 8.95$) [17]. In a similar manner to tetrabromobenzimidazole, the two brominated

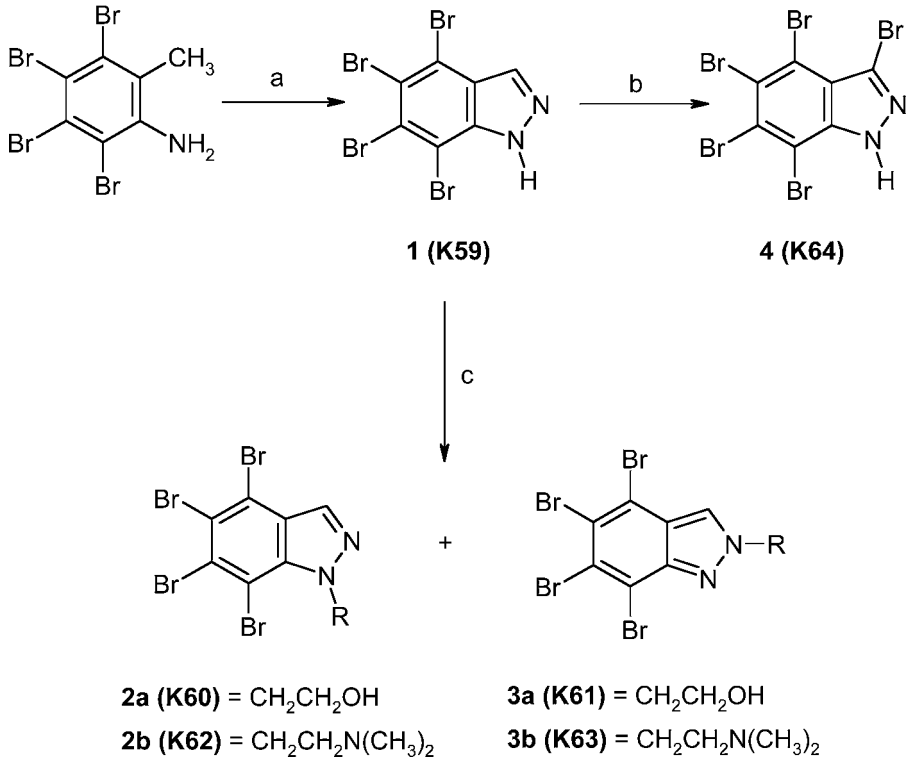

Scheme 1 Synthesis of substituted tetrabromoindazoles and pentabromoindazole

Reagents: (**a**) 1 = acetic oxide, 2 = nitrous gases (used sequentially); (**b**) Br_2, AcOH; (**c**) potassium carbonate, 2-butanone, 2-BrC_2H_4OH or $(CH_3)_2NCH_2CH_2Cl$.

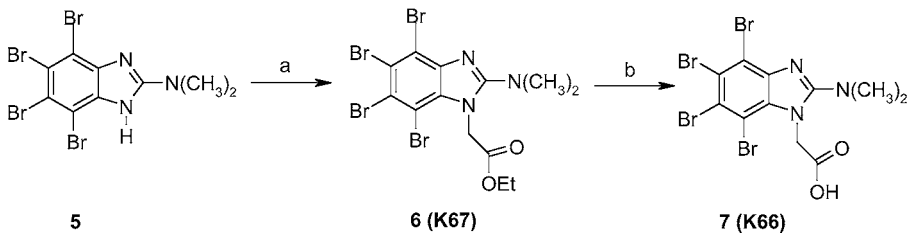

Scheme 2 Synthesis of 1-substituted derivatives of DMAT

Reagents: (**a**) K_2CO_3, acetone, $BrCH_2COOEt$; (**b**) 1 = NaOH, $EtOH/H_2O$, 2 = H^+ (used sequentially).

indazoles **1** and **4** described here are practically neutral molecules at physiological pH (Scheme 1).

The synthesis of 1-substituted acetic acid ethyl ester of 2-dimethylamino-4,5,6,7-tetrabromobenzimidazole **6** (K67) was performed by N-alkylation of DMAT (**5**) with bromoacetic acid ethyl ester in acetone in the presence of anhydrous potassium carbonate as base. The alkaline hydrolysis of **6** in ethanol/water solution gave the N^1-carboxymethyl derivative of DMAT (**7**, K66) (Scheme 2).

The other modified tetrabromobenzimidazoles were obtained from 1-methyl-4,5,6,7-tetrabromobenzimidazole (**8**) as substrate. The heating of **8** with thiourea in propan-1-ol gave the respective 2-mercapto derivative **9** (K72). Alkylation of **9** with bromoacetic acid ethyl ester yielded 2-sulfanylacetic acid ethyl ester **10**, which was substrate for further modifications. Aminolysis of **10** with methylamine gave the respective N-methylamide (**11**, K74), whereas alkaline hydrolysis yielded 1-methyl-4,5,6,7-tetrabromobenzimidazole-2-sulfanylacetic acid (**12**, K75). (Scheme 3).

A detailed description of the synthesis and analytical data for the newly obtained compounds discussed in the present study is shown in Supplementary Table S1 at http://www.BiochemJ.org/bj/415/bj4150353add.htm. The profiling of a library of compounds on CK2, PIM1 and HIPK2 is shown in Supplementary Table S2 at http://www.BiochemJ.org/bj/415/bj4150353add.htm.

RESULTS

Re-evaluation of TBB, DMAT and TBI selectivity

TBB and its 2-dimethylamino derivative DMAT are among the most widely used commercially available inhibitors of CK2. In contrast with other compounds used to inhibit CK2, notably DRB (5,6-dichloro-1-β-D-ribofuranosylbenzimidazole) and apigenin, both TBB and DMAT are believed to be very specific based on selectivity profiles run on panels of 30 and 33 protein kinases respectively [18,19]. More recently, however, the size of the

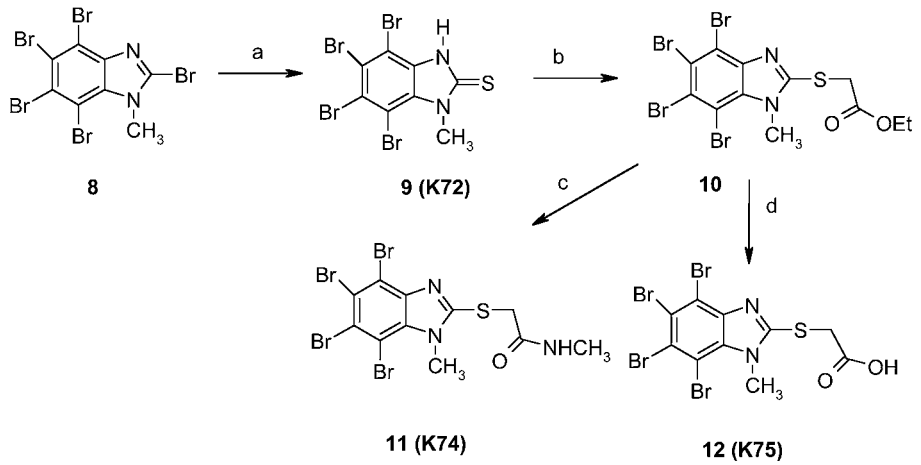

Scheme 3 Synthesis of 1-methyl-4,5,6,7-tetrabromobenzimidazole derivatives

Reagents: (**a**) thiourea, 1-PrOH; (**b**) K_2CO_3, acetone, $BrCH_2COOEt$; (**c**) NH_2CH_3, EtOH; (**d**) 1 = NaOH, EtOH/H_2O, 2 = H^+ (used sequentially).

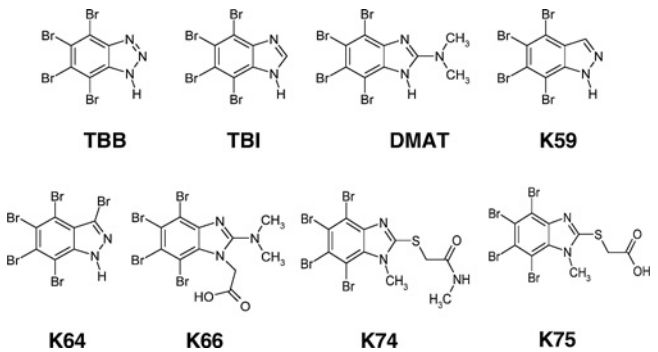

Figure 2 Molecular structure of representative benzotriazole, benzimidazole and benzopyrazole derivatives used in the present study

panel of kinases available for testing the specificity of inhibitors has more than doubled [22], so that currently this includes representatives of nearly all subfamilies of the kinome (Figure 1). This prompted us to re-evaluate the selectivity of TBB and DMAT toward CK2. Since DMAT shares its benzimidazole scaffold with the parent compound TBI (or TBBz) (see Figure 2) which is also marketed as a CK2 inhibitor (although its selectivity has not been profiled before), TBI was also included in the analysis in the present study.

The residual activity of a panel of 76 protein kinases tested in the presence of 10 μM TBB, DMAT and TBI and expressed as the percentage of their activity in the absence of inhibitors is reported in Table 1 or in the legend of Table 1. Even a cursory scrutiny of the data reveals that CK2 is not the only protein kinase drastically affected, several other kinases (values shown in bold in Table 1) are more than 90% inhibited by one or more of the three compounds. A more detailed analysis allows the following conclusions to be reached. (i) Although the selectivity spectra of TBB, DMAT and TBI are similar they are not superimposable, denoting higher similarity between DMAT and TBI (characterized by an imidazole ring), both of which also tend to be more promiscuous than TBB (composed instead of a triazole ring). This point is highlighted by drastic inhibition of PKD1 and CDK (cyclin-dependent kinase) 2/cyclin A by either DMAT or TBI, in contrast with fairly high residual activity observed in the presence of the same concentration of TBB. (ii) There are three subfamilies of protein kinases, none of which was represented in the 30 protein kinase panel originally used to define the TBB specificity [18], whose components tend to be inhibited as drastically as CK2 by all of the three compounds at a 10 μM concentration, with residual activities below 10%; these are DYRKs (1a, 2 and 3), PIMs (1, 2, 3) and HIPK2. A >90% inhibition of HIPK3 is also observed by DMAT and TBI, whereas TBB is significantly less effective in this respect.

More detailed information regarding the relative efficiency of each inhibitor toward protein kinases whose activity is 90% or more inhibited by a 10 μM concentration of inhibitor was obtained by determining their IC_{50} values at 50 μM ATP. These results are reported in Table 2 and they strengthen the notion that among the three inhibitors the most selective inhibitor towards CK2 was TBB with an IC_{50} value (0.15 μM) 3–5-fold lower than those of DYRK2, PIM1 and PIM3, and one order of magnitude or more below those of the other kinases. In contrast, TBI appears to be the least selective toward CK2, as it inhibits PIM3, PIM1, PIM2, DYRK2 and PDK1 more efficiently than CK2 itself, and HIPK2 and CDK2 with comparable efficiency. This is partially also due to its relatively high IC_{50} value with CK2 (0.60 μM).

The overall superiority of TBB over DMAT is also highlighted by selectivity profiles performed with a 1 μM instead of 10 μM inhibitor concentration (last two columns on the right in Table 1). Under these conditions the number of protein kinases inhibited by $\geqslant$50% are three and 12 with TBB and DMAT respectively (values shown as underlined in Table 1). Note that seven out of the 12 protein kinases that are $\geqslant$50% inhibited by DMAT are inhibited as drastically as CK2 itself.

DMAT as a powerful inhibitor of kinases other than CK2

Although the IC_{50} value with CK2 is quite low (0.13 μM), DMAT displays submicromolar IC_{50} values with almost all of the other kinases in Table 2, with special reference to PKD1, PIM3 and PIM1 whose IC_{50} value (148 nM) is comparable with that of the most potent PIM1 inhibitor [BIM-1 (bisindolylmaleimide)] reported to date [36].

In a similar manner to CK2 [19], PIM1 is also inhibited by DMAT by a mechanism which is competitive with respect to ATP, as shown by the double reciprocal plot shown in Figure 3(A). However, IC_{50} determinations at increasing ATP concentration denote weak competition by ATP which, at almost physiological

Table 1 Selectivity profiles of TBB, DMAT and K17 on a large kinase panel

Activity assays were linear with respect to time and enzyme concentration and were performed as previously described [22]. Residual activity was determined in the presence of the indicated concentrations of inhibitor and expressed as a percentage of the control without inhibitor. Residual activities $\leqslant$10% with 10 μM inhibitor are shown in bold, and those $\leqslant$50% with 1 μM inhibitor are underlined. Other protein kinases not included in the selectivity panel, namely the isoforms α, γ and δ of CK1, the tyrosine kinases Lyn, c-Fgr and Syk, and the G-CK (Golgi CK), were tested under conditions specified previously [18] and found to be unaffected ($<$10% inhibited) by 10 μM TBB, DMAT and TBI. AMPK, AMP-activated protein kinase; BRSK, brain-specific kinase; CaMK, calmodulin-dependent kinase; CaMKK, CaMK kinase; CHK, checkpoint kinase; CSK, C-terminal Src kinase; EFK, elongation factor kinase; GSK, glycogen synthase kinase; IKK, inhibitory κB kinase; JNK, c-Jun N-terminal kinase; Lck, lymphocyte cell-specific protein-tyrosine kinase; MAPK, mitogen-activated protein kinase; MAPKAP-K, MAPK-activated protein kinase; MARK, microtubule-affinity-regulating kinase; MELK, maternal embryonic leucine-zipper kinase; MKK, MAPK kinase; MNK, MAPK-integrating protein kinase; MST, mammalian homologue Ste20-like kinase; NEK, NIMA (never in mitosis in *Aspergillus nidulans*)-related kinase; PAK, p21-activated protein kinase; PHK, phosphorylase kinase; PKA, protein kinase A; PKB, protein kinase B; PKC, protein kinase C; PLK, polo-like kinase; PRAK, p38-regulated activated kinase; PRK, protein kinase C-related kinase; ROCK, Rho-dependent protein kinase; RSK, p90 ribosomal S6 kinase; S6K, S6 kinase; SGK, serum- and glucocorticoid-induced kinase; SmMLCK, smooth-muscle myosin light-chain kinase; Src, sarcoma kinase; SRPK, serine-arginine protein kinase.

Number	Kinase	TBB (10 μM)	DMAT (10 μM)	TBI (TBBz) (10 μM)	TBB (1 μM)	DMAT (1 μM)
1	MKK1	41	32	30	95	43
2	ERK1	106	78	78	91	96
3	ERK2	96	71	79	96	85
4	JNK1	33	66	42	91	84
5	JNK2	29	70	62	101	98
6	JNK3	52	85	68	100	95
7	p38α MAPK	100	79	88	83	81
8	P38β MAPK	96	89	89	98	94
9	p38γ MAPK	24	57	54	105	92
10	p38σ MAPK	100	66	67	98	107
11	ERK8	15	13	11	92	27
12	RSK1	63	29	36	102	91
13	RSK2	59	41	59	98	81
14	PDK1	86	76	81	94	100
15	PKBα	41	66	53	93	88
16	PKBβ	66	88	81	103	99
17	SGK1	30	24	16	100	73
18	S6K1	26	37	34	106	79
19	PKA	45	76	75	86	80
20	ROCK 2	58	42	31	90	90
21	PRK2	74	59	47	104	88
22	PKCα	84	87	92	93	95
23	PKCζ	37	40	44	79	62
24	PKD1	37	**10**	**5**	83	27
25	MSK1	36	29	24	107	90
26	MNK1	31	41	33	90	79
27	MNK2	30	30	33	103	68
28	MAPKAP-K2	64	90	74	96	90
29	MAPKAP-K3	72	94	94	107	99
30	PRAK	51	82	52	84	81
31	CAMKKα	71	84	68	116	118
32	CAMKKβ	26	44	48	76	73
33	CAMK1	101	42	25	101	96
34	SmMLCK	28	31	11	95	73
35	PHK	56	35	25	98	83
36	CHK1	105	71	70	85	82
37	CHK2	82	33	16	113	83
38	GSK3β	31	35	41	80	73
39	CDK2-Cyclin A	48	18	23	102	94
40	PLK1	25	41	29	88	81
41	PLK1 (okadaic acid)	14	39	34	90	78
42	AURORA B	47	17	15	85	67
43	AURORA C	41	28	24	73	76
44	AMPK	71	54	45	100	119
45	MARK3	68	58	47	99	85
46	BRSK2	72	55	24	72	63
47	MELK	47	36	43	79	70
48	CK1	61	80	48	95	100
49	CK2	**6**	**7**	**10**	21	19
50	DYRK1A	**4**	**5**	**3**	51	21
51	DYRK2	**3**	**6**	**9**	68	24
52	DYRK3	**4**	**3**	**6**	76	35
53	NEK2a	118	94	74	101	103
54	NEK6	63	105	79	108	142
55	NEK7	61	96	68	113	107
56	IKKβ	58	35	37	89	60
57	PIM1	**2**	**1**	**2**	27	**3**
58	PIM2	**7**	**6**	**2**	77	32

Table 1 (*Contd.*)

Number	Kinase	TBB (10 μM)	DMAT (10 μM)	TBI (TBBz) (10 μM)	TBB (1 μM)	DMAT (1 μM)
59	PIM3	**1**	**1**	**2**	**10**	**5**
60	SRPK1	55	70	76	93	98
61	MST2	63	45	35	102	90
62	EFK2	91	84	70	86	78
63	HIPK2	**5**	**2**	**3**	94	20
64	HIPK3	18	**6**	**9**	103	40
65	PAK4	71	70	58	95	89
66	PAK5	71	64	72	94	93
67	PAK6	75	96	93	94	103
68	Src	93	93	95	115	105
69	Lck	91	87	79	99	88
70	CSK	84	86	83	101	96

Table 2 IC_{50} (μM) of selected protein kinases for TBB, DMAT and TBI (TBBz)

Phosphorylation conditions are either as described in the Experimental section or as described previously [22]. The ATP concentration was 50 μM. Data with CK2 were obtained using native holoenzyme purified from rat liver. Replacement of native CK2 with recombinant human CK2 holoenzyme ($\alpha_2\beta_2$) or with the isolated α subunit caused only minor alterations in the IC_{50} values.

Kinase	TBI	DMAT	TBB
CK2	0.60	0.13	0.15
PIM1	0.115	0.148	1.04
PIM2	0.18	1.6	4.3
PIM3	0.07	0.097	0.86
HIPK2	0.7	0.37	5.3
HIPK3	1.22	0.59	4.9
DYRK1a	2.1	0.41	4.36
DYRK2	0.34	0.35	0.99
DYRK3	3.7	1.7	5.3
PKD1	0.34	0.18	5.9
CDK2	0.58	0.64	14.0

concentration (0.6 mM), causes only a 5.3-fold decrease in DMAT inhibition, as compared with 1 μM ATP concentration, whereas in the same range of ATP concentration the IC_{50} with CK2 increases 22.1-fold, doubling the value calculated with PIM1 (1.2 μM) (Figure 3B). Therefore it is expected that in the cellular environment (where ATP $\geqslant$1 mM), PIM1 will represent the preferred target of DMAT, among all of the protein kinases probed in this respect.

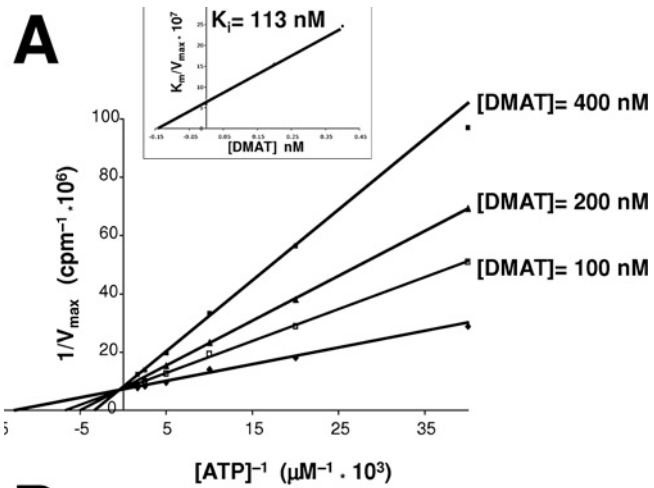

B

	PIM1 (IC_{50}, μM)	CK2 (IC_{50}, μM)
ATP 1 μM	0.11	0.056
ATP 25 μM	0.14	0.14
ATP 80 μM	-	0.34
ATP 100 μM	0.32	-
ATP 600 μM	0.60	1.24

Figure 3 Kinetic analysis of PIM-1 inhibition by DMAT

Phosphorylation assays were performed as described in the Experimental section in the absence and presence of the indicated concentrations of DMAT. The data represent the means of values obtained in triplicate with the S.D. never exceeding 15%. Lineweaver–Burk double reciprocal plots obtained in the absence and in the presence of the indicated DMAT concentrations are shown in (**A**). The inset refers to the K_m/V_{max} versus inhibitor concentration replot from which the value of K_i has been determined. (**B**) IC_{50} values for the inhibition of PIM1 and CK2 by DMAT calculated at increasing ATP concentrations.

Improvement of selectivity toward CK2

The observation that CK2 inhibitors tend to inhibit with comparable efficacy at least three other groups of kinases, notably PIMs, HIPK2 and DYRKs, prompted us to search for more selective compounds in the available library of TBB/TBI derivatives. This presently includes, besides several dozens of tetrabromobenzimidazole congeners previously described [19,32], also a number of newly developed compounds with a pyrazole penta-atomic ring replacing for the imidazole ring, whose prototype K59 is shown in Figure 2 together with its triazole (TBB) and imidazole (TBI) congeners. All of the compounds of the library (68 altogether) were tested at a 20 μM concentration on CK2, PIM1 and HIPK2. The assays were run at ATP concentrations at approx. the K_m values of the kinases (20 μM for CK2 and HIPK2, 100 μM for PIM1) and the residual activities are shown in Supplementary Table S2 .

Focusing our attention only on compounds highly effective on CK2 (residual activity $\leqslant$15%, shown in bold in Supplementary Table S2) we observed that most of these are equally, or even more, potent inhibitors of PIM1, and two actually inhibit HIPK2 even more efficiently than CK2. A few compounds, however, namely K36, K59, K60, K62, K64, K66, K74 and K75, whose structures are shown in Table 3, displayed an inhibitory efficacy

Table 3 K_i values (μM) of selected compounds for CK2, PIM1, HIPK2 and DYRK1a protein kinases

Kinetic determinations were performed as described in the Experimental section (with native CK2 holoenzyme) according to the Cheng–Prusoff equation [28].

Kinase	K36	K59	K60	K62	K64	K66	K74	K75
CK2	0.08	0.068	0.71	0.40	0.048	0.25	0.28	0.16
PIM1	0.56	0.55	3.66	4.50	0.738	8.65	4.00	2.55
HIPK2	2.29	1.53	11.33	8.88	1.594	15.25	60.31	12.77
DYRK1a	>25.00	1.00	3.45	2.85	1.64	11.90	>40.00	12.10

significantly higher towards CK2 than those observed with either PIM1 or HIPK2.

The K_i values of these compounds with respect to CK2, PIM1, HIPK2 and DYRK1a were calculated (Table 3). In all cases CK2 displayed the lowest K_i value as compared with the other three protein kinases. In particular two compounds, K59 and K64 displayed K_i values below 100 nM with CK2, whereas their K_i values with the second most sensitive protein kinase, which is PIM1 in both cases, were several-fold higher. Both K59 and K64 are characterized by a pyrazole ring replaced for the triazole/imidazole rings of TBB and DMAT. K64 also contains a fifth bromine atom on the pyrazole ring in addition to the four bromine atoms on the benzene ring which are a common denominator of all TBB derivatives described so far. Three other promising compounds belong to the benzimidazole class: these are K66, K74 and K75. In this case the K_i calculated with CK2 was somewhat higher than 100 nM: this disadvantage however is amply compensated by proportionally higher K_i values with PIM1, HIPK2 and DYRK1a. We focused further attention on those compounds whose K_i values with CK2 were 10-fold or more lower than those with the second most inhibited kinase, notably K64, K66, K74 and K75.

We first investigated whether, and to what extent, the double mutation of CK2 residues Val[66] and Ile[174] to alanine residues, previously reported to decrease susceptibility to TBB and DMAT [19,20], also affected inhibition by the new compounds. This is clearly the case, as shown in Table 4; however, responsiveness to the double mutation was sharply variable: two inhibitors, K74 and K75, were somewhat more sensitive than TBB and DMAT to the double mutation, whereas K66 was almost insensitive to it, with a just 6-fold increase in IC_{50} value. By sharp contrast the pentabrominated inhibitor K64 had lost almost all of its efficacy toward the CK2 double mutant, with a 600-fold increase in IC_{50}. These differences clearly reflect diverse modes of binding of these compounds, as further indicated by the variable efficacy of the two single mutations, that of Val[66] and of Ile[174]. In particular the role of Ile[174] is crucial for the binding of K64, whereas the binding of K66 relies more on interactions with Val[66] as also confirmed by modelling (see Discussion below).

The behaviour of K66 attracted our attention because its scaffold is identical with that of DMAT, having in addition a short carboxylic side chain adjacent to the imidazole ring nitrogen (compare structures in Figure 2). Although this carboxylic adduct is still compatible with fairly potent inhibition of CK2 it makes its binding almost independent of Ile[174], whereas it is more dependent on Val[66] (Table 4), and, more importantly, it drastically reduces the ability of K66 to inhibit PIM1 and HIPK2 which are instead dramatically sensitive to DMAT (see Table 2).

Table 4 IC_{50} (μM) of selected indazole and benzimidazole derivatives for wild-type and mutated CK2

Recombinant CK2 holoenzyme was reconstituted *in vitro* by mixing at a 1:1 molar ratio the β-subunit with wild-type or the mutated CK2α subunit. The data represent the mean of three independent experiments with the S.D. never exceeding 12%. dm = double mutant in which both Val[66] and Ile[174] have been replaced by alanine; wt, wild-type.

Compound	CK2 wt	V66A	I174A	CK2 dm	Ratio dm/wt
K64	0.052	2.60	>40.00	31.28	601.5
K66	0.50	22.37	1.14	3.32	6.6
K74	0.60	>40.00	>40.00	40.64	67.3
K75	0.31	40.00	>40.00	15.22	49.0
DMAT*	0.14	1.78	3.30	5.79	30.47

*Data obtained from [19].

Once we ascertained that the new CK2 inhibitors considered in Table 3, with special reference to K64, K66 and K75, had lost most of their potency toward those protein kinases which display the tendency of being susceptible to CK2 inhibitors, notably PIM1, HIPK2 and DYRK1a, we wanted to make sure that their overall selectivity was preserved. This analysis was performed on a panel of 78 protein kinases almost completely, but not entirely, overlapping the panel of 70 protein kinases used for the screening presented in Table 1. The results are shown in Figure 4. For the sake of comparison, the results relative to DMAT are reported. The most remarkable outcome is indeed the dramatic gain of selectivity resulting from the derivatization of DMAT with a carboxymethyl side chain to give K66 (Figure 4), whereas, as noted above, DMAT under these conditions inhibits by $\geqslant 50\,\%$ 34 kinases out of 70 (i.e. almost 50%), this figure with K66 drops to just five kinases out of 78. Only two of these, not including CK2, are drastically inhibited ($\geqslant$80%) by K66: ERK (extracellular-signal-regulated kinase) 8 and DYRK2. However, the IC_{50} values for inhibition of DYRK2 is far above that of CK2 (8 μM as compared with 0.25, see the legend of Figure 4). Consequently the only kinase whose inhibition by K66 is comparable with that of CK2 is ERK8 ($IC_{50} = 0.50\ \mu$M), thus placing K66 in the category of 'dual-kinase inhibitors' able to block with equal efficiency two unrelated kinases. Note in this respect that it would be easy to discriminate between ERK8 and CK2 using the inhibitor BAY439006 which at 10 μM concentration suppresses ERK8 activity without significantly affecting CK2 [27].

The overall selectivity of K64 (Figure 4) is also good, with six protein kinases (including CK2) inhibited by $\geqslant$50% with 10 μM of inhibitor. One of these is again ERK8, but in this case it is inhibited significantly less than CK2. The same applies to PIM2,

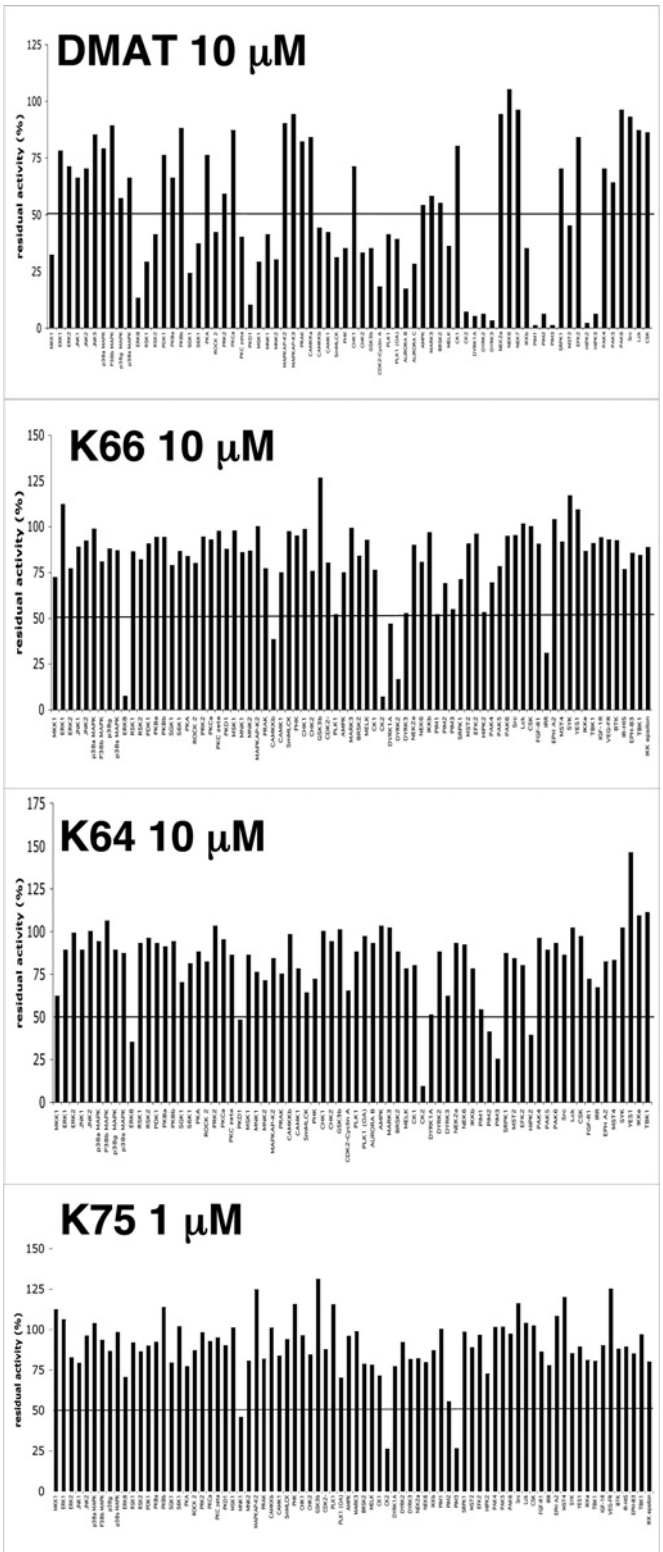

Figure 4 Comparison between the selectivity profiles of DMAT and some new CK2 inhibitors

Activity assays were linear with respect to time and enzyme concentration and were performed as described previously [22]. Residual activity was determined in the presence of 10 μM inhibitor except in the case of K75 which was tested at 1 μM (see the text for details) and expressed as a percentage of the control without inhibitor. DMAT is also shown for comparison (data drawn from Table 1). IC_{50} values of K66, determined for ERK8 and DYRK2, were 0.5 and 8 respectively.

PIM3, HIPK2 and PKD1, whose IC_{50} values accordingly are at least one order of magnitude higher than that of CK2.

Owing to solubility problems, the selectivity of K75 was profiled at a 1 μM concentration (Figure 4). Under these conditions only three kinases were inhibited by $\geqslant$50%: CK2 and PIM3 (both 70% inhibited), and MSK1 (mitogen- and stress-activated protein kinase 1; 54% inhibited).

K74 turned out to be unstable when kept for >2 h in DMSO solution, a circumstance which prevented its robotic profiling on the panel of protein kinases and probably also seriously hampers its usage in cell experimentation.

Pro-apoptotic efficacy of K64 and K66

In light of the results presented above the first-choice novel CK2 inhibitors worthy to be tested on cell cultures were K64 and K66, whose selectivity is comparable. The former is somewhat more potent but the latter has the advantage that its only known target inhibited as drastically as CK2, ERK8, is absent in haematopoietic cells [37], which are those most frequently used for testing the pro-survival and oncogenic potential of CK2 (e.g. [16,38–40]). An added value of K64 is instead its almost complete loss of efficacy toward the CK2 double mutant V66A/I174A (see Table 4), a property which can be exploited to provide the proof-of-concept that the cellular effects of a given inhibitor are actually mediated by CK2 rather than by other cellular targets.

As shown in Figure 5(A) both K64 and K66 displayed cytotoxic activity comparable with that of TBB. Interestingly the cytotoxic efficacy of the three compounds approx. correlates to their potency as CK2 inhibitors calculated from their K_i values (0.048, 0.12 and 0.25 for K64, TBB and K66 respectively). It should also be noted that although in principle the cytotoxic effect of TBB could be accounted for by the inhibition of protein kinases of the PIM and DYRK families having IC_{50} values close to that of CK2 (Table 2), this does not apply to K64 and K66 (see above). As shown in Figure 5(B) the cytotoxic effect of K64, similar to that of TBB [40] and of K66 is, at least partially, due to apoptosis as judged from the quantification of nucleosomes present in the cytosol of the apoptotic cells: nucleosomes in cells treated with 5 μM K64 are comparable with those induced by 25 μM etoposide.

DISCUSSION

Considering that the human kinome is composed of more than 500 members whose catalytic site is highly conserved and that the most promising cell-permeable protein kinase inhibitors are competitive with respect to the universal kinase co-substrate ATP, it is understandable that the development of really specific protein kinase inhibitors is a formidable challenge. Although absolute selectivity may be not required for a kinase inhibitor to become a valuable drug and some promiscuity could even be an advantage in terms of therapeutic efficacy, as exemplified by clinical practice with Imatinib/Gleevec [41], lack of specificity is always a serious drawback whenever inhibitors are used to dissect the biological functions of a given protein kinase, where the unwanted blockage of other kinases may generate misleading results. This shortcoming can be attenuated by using more than one inhibitor of the same kinase and can be circumvented by the generation and cell transfection of kinase mutants which are refractory to a given inhibitor. Since, however, clusters of kinases often tend to be inhibited by the same classes of inhibitors and cell transfection is not always feasible and is likely to alter cell functionality anyway, the availability of pharmacological tools that are as selective as possible invariably represents a critical

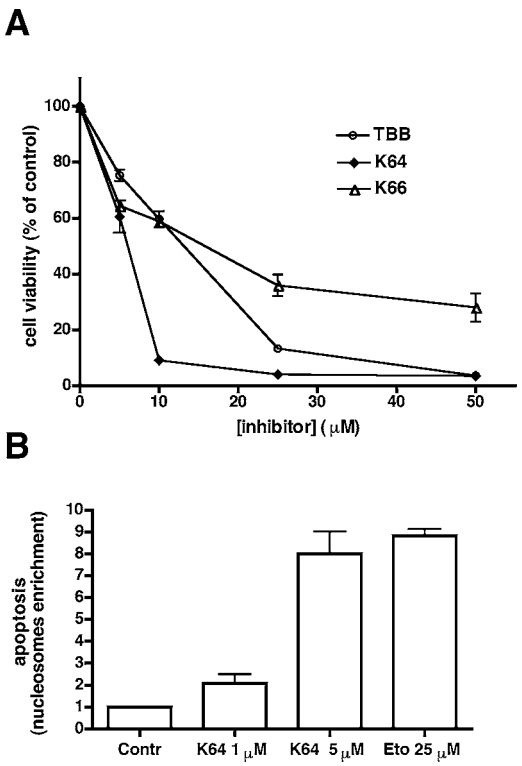

Figure 5 Pro-apoptotic efficacy of new CK2 inhibitors on Jurkat cells

(**A**) Jurkat cells were treated for 24 h with increasing concentrations of the indicated inhibitors. Cell viability was assessed by the MTT method, assigning 100% value to the control cells, treated with the solvent. Reported values represent the means ± S.E.M. from four separate experiments. (**B**) Jurkat cells were treated with the indicated concentrations of inhibitor for 4 h. Apoptosis was evaluated by quantification of nucleosomes present in the cytosol of the apoptotic cells, using the Cell Detection Elisa kit (Roche). Treatment with 25 μM etoposide (Eto) was used as a positive control for apoptosis induction. Nucleosome enrichment was calculated from the ratio between the signal in control cells and treated cells.

advantage for dissecting signalling pathways. This is especially true in the case of protein kinases such as CK2 which are constitutively active and cannot be easily up- or down-regulated within the cell using physiological effectors.

In the past considerable efforts have been made to develop CK2-specific inhibitors, belonging to different chemical classes (reviewed by Sarno et al. [13,14]). Apart from apigenin, a flavonoid devoid of narrow selectivity [20,42], the two most successful CK2 inhibitors were both derived from the nucleoside DRB, a rather weak CK2 inhibitor [43], by deleting its sugar moiety and replacing the chlorine and hydrogen atoms of its benzene ring with four bromine atoms. These were shown to be critical to encapsulate the inhibitor in a hydrophobic cavity which in CK2 is smaller than in the majority of other protein kinases [24,25]. This feature, which underlies the fairly narrow selectivity of these compounds toward CK2, has been exploited in many recent reports to probe the implication of this kinase in a variety of cellular functions [10]. However, despite their structural similarity TBB and DMAT bind in different ways into the active site of CK2 [25], denoting a role of the negative charge present at neutral pH on the triazole ring of TBB, which is not present in DMAT or in the other TBB derivatives [17,23]. In the latter the N^2 atom is replaced by a carbon, to give a tetrabromobenzimidazole derivative (TBI or TBBz) devoid of the negative charge at neutral pH [17]. The relevance of this difference to determine kinase selectivity was overlooked in our original studies because the panel of kinases used at that time for selectivity profiles was not large enough to disclose significant differences. It was concluded therefore that, apart from some minor differences, TBB and DMAT exhibited quite super-imposable inhibition profiles and a similar, quite remarkable, selectivity toward CK2, although DMAT is somewhat more potent, especially if used in cell culture [44]. Another advantage of DMAT, as well as of TBI and the other benzimidazole derivatives analysed in this respect [23] is that, owing to its high pK_a value (8.9 for TBI and 10.6 for DMAT), at physiological pH the N-H of the imidazole ring is not dissociable and therefore these compounds are unable to depolarize mitochondria [19] by shuttling protons across the membrane. The same applies to the pyrazole ring of the indazole derivatives, e.g. K59 (p$K_a = 10.6$) and K64 (p$K_a = 8.40$) (see the Experimental section). In contrast, mitochondria depolarization is a drawback of TBB [20] whose triazole ring exhibits a much lower pH value, allowing proton shuttling under the effect of the pH gradient on the two sides of the mitochondrial membrane.

In the present study, exploiting a panel of kinases more than twice as large as the original one, and including members of nearly all of the kinome subfamily (Figure 1), we have reached the conclusion that the selectivity of TBB is definitely narrower than that of DMAT and TBI. Although in fact both DMAT and TBI drastically inhibit several kinases in addition to CK2, notably PIM1, 2 and 3, DYRK1a, 2 and 3, PKD1, HIPK2 and 3, and CDK/CyclinA, TBB is significantly less effective on these kinases than it is on CK2 as highlighted by comparing both IC_{50} values (Table 2) and selectivity profiles of TBB and DMAT performed at a 1 μM inhibitor concentration (see Table 1). On the other hand, the possibility should be considered that besides protein kinases non-kinase enzymes also interact with CK2 inhibitors: this applies to TBB, but, even more to TBI and DMAT [45].

The results of the present study provide valuable hints for the development of PIM and HIPK inhibitors more potent and/or selective than those currently available. In the case of PIM1, the product of a proto-oncogene whose dysfunction has been implicated in diverse cancers with special reference to DLCL (diffuse large cell lymphoma) [46], some inhibitors are available [36], whose potency is comparable with those of TBI and DMAT and whose selectivity has not been explored. Our results also provide the possibility to discriminate among PIM isoforms exploiting their different susceptibilities to TBI and DMAT (see Table 2). In contrast, inhibitors of HIPK2, a kinase required for normal haematopoiesis and blood vessel formation [47] which plays a critical role in triggering p53-dependent apoptosis in response to the anti-neoplastic drug cisplatin [48], are not available at all to the best of our knowledge, a circumstance which makes DMAT and TBI the best tools presently available to down-regulate HIPK2.

Once established that TBB and, even more, DMAT and TBI are CK2 inhibitors less selective than it was previously thought, our next aim was the identification of DMAT/TBB derivatives which are still effective on CK2 having lost most of their efficacy toward PIM1, HIPK2 and DYRK1a. This goal turned out to be hard to attain since most compounds tested, which are potent inhibitors of CK2, also tend to inhibit PIM1 and/or HIPK2 with similar potency (see Supplementary Table S2). A few notable exceptions, however, were provided by two compounds belonging to the class of indazoles (K59 and K64), having a pyrazole ring replaced for the triazole and imidazole pentatomic rings present in TBB and DMAT respectively, and three new benzimidazole derivatives (K66, K74 and K75). These are all characterized by the ability to inhibit CK2 more potently than PIM1, HIPK2 and DYRK1a, with K_i values which in the case of K64 and K66 are many-fold lower than those calculated with the second most inhibited kinase (PIM1 in both cases)

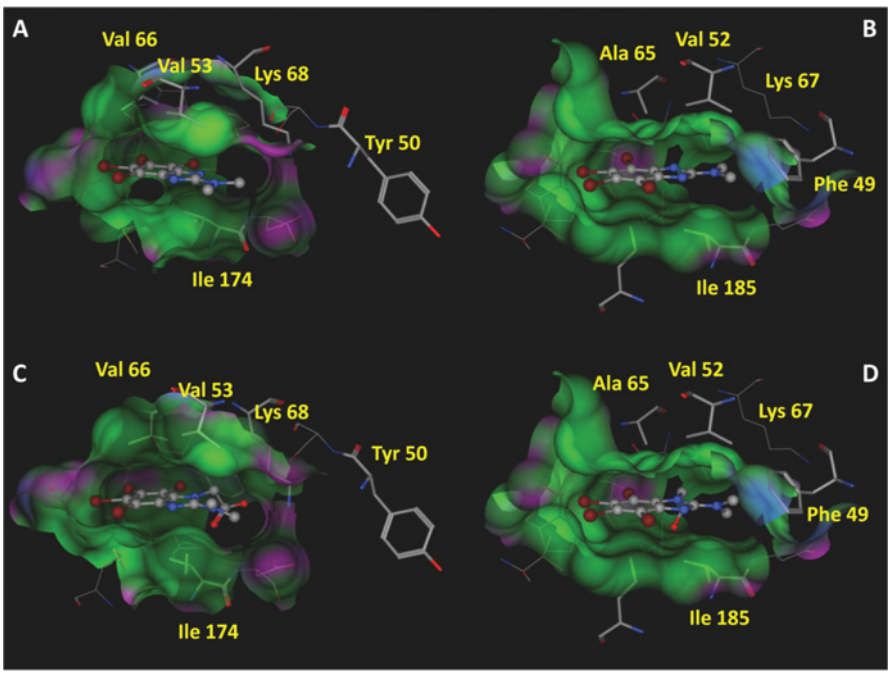

Figure 6 Molecular docking of DMAT (A and B) and K66 (C and D) bound to the active site of CK2 (left-hand side) and PIM1 (right-hand side)

Molecular docking was performed as described in the Experimental section. Active LonePair distribution surface of CK2- and PIM1-binding pockets were represented. Green indicates hydrophobic regions, whereas in violet are hydrogen bonding or metal–LonePair regions.

In this respect, the behaviour of K66 appears to be especially remarkable, considering its close structural relatedness with DMAT: while DMAT inhibits PIM1 with the same potency as CK2, K66 has lost most of its efficacy toward PIM1, as judged from big differences in K_i and IC_{50} values.

The structural similarity between DMAT and K66, in conjunction with the availability of three-dimensional structures of both PIM1 and CK2, the latter also in complex with DMAT [25], provide a key to rationalize the preferential binding of K66 to CK2. The structure of DMAT bound into the active site of CK2, together with the derived model in which DMAT has been replaced by K66 are shown in Figures 6(A) and 6(C). This accounts very well for the finding that Ile^{174} is less important for the binding of K66 (see Table 4). Note in fact that K66, owing to its carboxylic group, is making electrostatic interactions with the positive area close to Lys^{68} thus displacing the dimethylamino group from its apolar contacts with Ile^{174} and placing it closer to Val^{66}. In the case of PIM1, DMAT is rotated approx. 60° with respect to the crystallographic data, owing to the presence of Phe^{49}. In fact, unlike its CK2 homologue Tyr^{50} which is exposed toward the solvent, Phe^{49} is instead oriented toward the hydrophobic cavity forcing the inhibitor to a new pose. As shown in Figure 6(B) the dimethylamino group at position 2 is placed inside a new favourable hydrophobic pocket formed by PIM1 residues Val^{52}, Leu^{120}, Ile^{185} and Phe^{49}, whereas in CK2 it is simply oriented towards the outside (Figure 6A). These structural observations may explain the similar activity of DMAT in CK2 and PIM1, even in the presence of Val^{66}/Ala^{65} natural substitution. On the other hand, K66 interacts with the PIM1-binding cleft in the same way as shown for DMAT due to the presence of the dimethylamino group. Under these conditions its carboxy side chain at position 1 cannot interact with Lys^{67}, homologous with CK2 Lys^{68}, and therefore it is placed in an unfavourable hydrophobic zone (Figure 6D).

Importantly the improved selectivity of K66 as compared with DMAT is not restricted to its ability to discriminate between CK2 and PIM1, but it also reflects a reduced or abolished inhibitory efficiency towards a large number of kinases deeply affected by DMAT, as outlined by comparing their specificity profiles in Figure 4: although 34 kinases are inhibited by $\geqslant$50% at 10 μM DMAT, this figure drops to just five kinases with K66, under identical conditions. Only one of the latter (ERK8) is inhibited as drastically as CK2 (i.e. >80%), whereas 12 of those are >80% inhibited by DMAT.

In an attempt to quantify these differences a 'promiscuity score' has been devised, expressing the 'average' inhibition of all of the kinases of the whole panel, by a given concentration of the inhibitor, sufficient to drastically inhibit (approx. 90%) the kinase considered (in our case CK2) (see the legend of Table 5). Such a score, which reflects the promiscuity of the kinase and is inversely proportional to its 'average' selectivity, equals 18.36 and 46.66 with 10 μM K66 and DMAT respectively. Interestingly a promiscuity score similar to that of K66 has been calculated for K64 (16.8) reinforcing the concept that both K64 and K66 are markedly more selective than the three related commercially available CK2 inhibitors, TBB, DMAT and TBI, the latter having a score >50 (see Table 5). It should be also noted that, while at a 10 μM concentration of inhibitor the promiscuity scores of TBB and DMAT are similar, if the profiling is performed at a 1 μM concentration, where CK2 is approx. 80% inhibited by either TBB or DMAT (see Table 1), the promiscuity score of DMAT (23.1) doubles that of TBB (10.18) confirming also by this criterion the concept that TBB is more selective than DMAT. However, comparing the selectivity of TBB with those of K64 and K66 whose selectivity is much higher, and considering that the latter are equally effective as TBB as inducers of apoptosis it is predictable that K64 and K66 will replace TBB (although not DMAT and TBI) as the

Table 5 Promiscuity score of selected CK2 inhibitors

The promiscuity score was calculated from the selectivity profiles (Figure 4 and Table 1) as the mean of percentage inhibitions observed with all of the kinases tested, excluding the kinase of interest (CK2). Inhibition of CK2 was 93–95% in the presence of 10 μM inhibitors and 80% in the presence of 1 μM DMAT and TBB. Values of inhibition <0 (i.e. stimulation) were adjusted to 0%.

Inhibitor	Concentration (μM)	Score (%)
K64	10	17.00
K66	10	19.33
DMAT	10	48.60
TBB	10	47.37
DMAT	1	23.10
TBB	1	10.18

first choice tool for studying cellular functions of CK2. Since the chemical names of K64 and K66 are exceedingly long (3,4,5,6,7-pentabromo-1*H*-indazole and 4,5,6,7-tetrabromo-2-methylamino-1-carboxymethyl-benzimidazole respectively) we propose that, by analogy to TBB and DMAT, they are denoted by the acronyms PBIN and TMCB.

We thank Professor Sir Philip Cohen (MRC Protein Phosphorylation Unit, University of Dundee, Dundee, Scotland, U.K.) for critical reading of the manuscript. The Molecular Modelling Section co-ordinated by Professor Stefano Moro (University of Padova, Padova, Italy) is gratefully acknowledged. The work was supported by grants to L.A.P. from AIRC (Associazione Italiana per la Ricerca sul Cancro) and European Commission (PRO-KINASERESEARCH 503467) and by a grant to Z.K. and A.O. from the Ministry of Education and Science PBZ-MIN 014/P05/2004 (Poland).

REFERENCES

1 Meggio, F. and Pinna, L. A. (2003) One-thousand-and-one substrates of protein kinase CK2? FASEB J. **17**, 349–368
2 Pagano, M. A., Cesaro, L., Meggio, F. and Pinna, L. A. (2006) Protein kinase CK2: a newcomer in the 'druggable kinome'. Biochem. Soc. Trans. **34**, 1303–1306
3 Pinna, L. A. (2003) The raison d'etre of constitutively active protein kinases: the lesson of CK2. Acc. Chem. Res. **36**, 378–384
4 Litchfield, D. W. (2003) Protein kinase CK2: structure, regulation and role in cellular decisions of life and death. Biochem. J. **369**, 1–15
5 Stalter, G., Siener, S., Becht, E., Ziegler, M., Remberger, K. and Issinger, O.-G. (1994) Asymmetric expression of protein kinase CK2 subunits in human kidney tumors. Biochem. Biophys. Res. Commun. **202**, 141–147
6 Landesmann-Bollag, E., Romieu-Mourez, R., Song, D. H., Sonenshein, G. E., Cardiff, R. D. and Seldin, D. C. (2001) Protein kinase CK2 in mammary gland tumorigenesis. Oncogene **20**, 3247–3257
7 Daya-Makin, M., Sanghera, J. S., Mogentale, T., Lipp, M., Parchomchuk, J., Hogg, J. and Pelech, S. (1994) Activation of a tumour-associated protein kinase (p40TAK) and casein kinase II in human squamous cell carcinomas and adenocarcinomas of the lung. Cancer Res. **54**, 2262–2268
8 Faust, R. A., Tawfic, S. and Davis, A. (2000) Antisense oligonucleotides against protein kinase CK2-α inhibit growth of squamous cell carcinoma of the head and neck *in vivo*. Head Neck **22**, 341–346
9 Yenice, S., Davis, A. T., Goueli, S. A., Akdas, A., Limas, C. and Ahmed, K. (1994) Nuclear casein kinase 2 (CK2) activity in human normal, benign hyperplastic and cancerous prostate. Prostate **24**, 11–16
10 Duncan, J. S. and Litchfield, D. W. (2008) Too much of a good thing: the role of protein kinase CK2 in tumorigenesis and prospects for therapeutic inhibition of CK2. Biochim. Biophys. Acta **1784**, 33–47
11 Wang, G., Unger, G., Kashif, A., Ahmad, A., Slaton, J. W. and Ahmed, K. (2005) Downregulation of CK2 induces apoptosis in cancer cells: a potential approach to cancer therapy. Mol. Cell. Biochem. **274**, 77–84
12 Seeber, S., Issinger, O.-G., Holm, T., Kristensen, L. P. and Guerra, B. (2005) Validation of protein kinase CK2 as oncological target. Apoptosis **10**, 875–885
13 Sarno, S., Ruzzene, M., Frascella, P., Pagano, M. A., Meggio, F., Zambon, A., Mazzorana, M., Di Maira, G., Lucchini, V. and Pinna, L. A. (2005) Development and exploitation of CK2 inhibitors. Mol. Cell. Biochem. **274**, 69–76
14 Sarno, S., Salvi, M., Battistutta, R., Zanotti, G. and Pinna, L. A. (2005) Features and potentials of ATP-site directed CK2 inhibitors. Biochim. Biophys. Acta **1754**, 263–270
15 Loizou, J. I., El-Khamisy, S. F., Zlatanou, A., Moore, D. J., Chan, D. W., Qin, J., Sarno, S., Meggio, F., Pinna, L. A. and Caldecott, K. W. (2004) The protein kinase CK2 facilitates repair of chromosomal DNA single-strand breaks. Cell **117**, 17–28
16 Piazza, F. A., Ruzzene, M., Gurrieri, C., Montini, B., Bonanni, L., Chioetto, G., Di Maira, G., Barbon, F., Cabrelle, A., Zambello, R. et al. (2006) Multiple myeloma cell survival relies on high activity of protein kinase CK2. Blood **108**, 1698–1707
17 Zien, P., Duncan, J. S., Skierski, J., Bretner, M., Litchfield, D. W. and Shugar, D. (2005) Tetrabromobenzotriazole (TBBt) and tetrabromobenzimidazole (TBBz) as selective inhibitors of protein kinase CK2: evaluation of their effects on cells and different molecular forms of human CK2. Biochim. Biophys. Acta **1754**, 271–280
18 Sarno, S., Reddy, H., Meggio, F., Ruzzene, M., Davies, S. P., Donella-Deana, A., Shugar, D. and Pinna, L. A. (2001) Selectivity of 4,5,6,7-tetrabromobenzotriazole, an ATP site-directed inhibitor of protein kinase CK2 ('casein kinase-2'). FEBS Lett. **496**, 44–48
19 Pagano, M. A., Andrzejewska, M., Ruzzene, M., Sarno, S., Cesaro, L., Bain, J., Elliott, M., Meggio, F., Kazimierczuk, Z. and Pinna, LA. (2004) Optimization of protein kinase CK2 inhibitors derived from 4,5,6,7-tetrabromobenzimidazole. J. Med. Chem. **47**, 6239–6247
20 Sarno, S., De Moliner, E., Ruzzene, M., Pagano, M. A., Battistutta, R., Bain, J., Fabbro, D., Schoepfer, J., Elliott, M., Furet, P. et al. (2003) Biochemical and 3D-structural data on the specific inhibition of protein kinase CK2 by [5-oxo-5,6-dihydro-indolo(1,2-a)quinazolin-7-yl]acetic acid (IQA). Biochem. J. **374**, 639–646
21 Davies, S. P., Reddy, H., Caivano, M. and Cohen, P. (2000) Specificity and mechanism of action of some commonly used protein kinase inhibitors. Biochem. J. **351**, 95–105
22 Bain, J., Plater, L., Elliott, M., Shpiro, N., Hastie, J., McLauchlan, H., Klevernic, I., Arthur, S., Alessi, D. and Cohen, P. (2007) The selectivity of protein kinase inhibitors; a further update. Biochem. J. **408**, 297–315
23 Battistutta, R., Mazzorana, M., Cendron, L., Bortolato, A., Sarno, S., Kazimierczuk, Z., Zanotti, G., Moro, S. and Pinna, L. A. (2007) The ATP-binding site of protein kinase CK2 holds a positive electrostatic area and conserved water molecules. Chembiochem **8**, 1804–1809
24 Battistutta, R., De Moliner, E., Sarno, S., Zanotti, G. and Pinna, L. A. (2001) Structural features underlying selective inhibition of protein kinase CK2 by ATP site-directed tetrabromo-2-benzotriazole. Prot. Sci. **10**, 2200–2206
25 Battistutta, R., Mazzorana, M., Sarno, S., Kazimierczuk, Z., Zanotti, G. and Pinna, L. A. (2005) Inspecting the structure–activity relationship of protein kinase CK2 inhibitors derived from tetrabromo-benzimidazole. Chem. Biol. **12**, 1211–1219
26 Meggio, F., Donella Deana, A. and Pinna, L. (1981) Endogenous phosphate acceptor proteins for rat liver cytosolic casein kinases. J. Biol. Chem. **256**, 11958–11961
27 Sarno, S., Vaglio, P., Meggio, F., Issinger, O.-G. and Pinna, L. A. (1996) Protein kinase CK2 mutants defective in substrate recognition. Purification and kinetic analysis. J. Biol. Chem. **271**, 10595–10601
28 Cheng, Y.-C. and Prusoff, W. H. (1973) Relationship between the inhibition constant (K1) and the concentration of inhibitor which causes 50 per cent inhibition (I50) of an enzymatic reaction. Biochem. Pharmacol. **22**, 3099–3108
29 Burlingham, T. B. and Widlanski, T. S. (2003) An intuitive look at the relationship of K_i and IC_{50}: a more general use of the Dixon plot. J. Chem. Ed. **80**, 214–218
30 Cozza, G., Bonvini, P., Zorzi, E., Poletto, G., Pagano, M. A., Sarno, S., Donella-Deana, A., Zagotto, G., Rosolen, A., Pinna, L. A. et al. (2006) Identification of ellagic acid as potent inhibitor of protein kinase CK2: a successful example of a virtual screening application. J. Med. Chem. **49**, 2363–2366
31 Szyszka, R., Grankowski, N., Felczak, K. and Shugar, D. (1995) Halogenated benzimidazoles and benzotriazoles as selective inhibitors of protein kinases CK I and CK II from *Saccharomyces cerevisiae* and other sources. Biochem. Biophys. Res. Commun. **208**, 418–424
32 Andrzejewska, M., Pagano, M. A., Meggio, F., Brunati, M. and Kazimierczuk, Z. (2003) Polyhalogenobenzimidazoles: synthesis and their inhibitory activity against casein kinases. Bioorg. Med. Chem. **11**, 3997–4002
33 Shishkin, V. N., Lapin, K. K., Tanaseichuk, B. S. and Butin, K. P. (1990) Polybromoaromatic compounds. V. Reaction of pentabromotoluene with sodium methoxide in pyridine. J. Org. Chem. USSR **26**, 2181–2188
34 Rousseau, H. G. and Lindwall, J. (1950) Structure and ultraviolet absorption spectra of indazole, 3-substituted indazole and some of their derivatives. Am. Chem. Soc. **72**, 3047–3051
35 Da Costa, M. R. G., Curto, M. J. M., Davies, S. G., Duarte, M. T., Resende, C. and Teixeira, F. C. (2000) Novel synthesis of indazoles from (η6-arene)tricarbonylchromium complexes. J. Organometall. Chem. **604**, 157–169
36 Bullock, A. N, Debreczeni, J. E., Fedorov, O. Y., Nelson, A., Marsden, B. D. and Knapp, S. (2005) Structural basis of inhibitor specificity of the human protooncogene proviral insertion site in moloney murine leukemia virus (PIM-1) kinase. J. Med. Chem. **48**, 7604–7614

37 Abe, M. K., Saelzler, M. P., Espinosa, 3rd, R., Kahle, K. T., Hershenson, M. B., Le Beau, M. M. and Rosner, M. R. (2002) ERK8, a new member of the mitogen-activated protein kinase family. J. Biol. Chem. **277**, 16733–16743
38 Mishra, S., Pertz, V., Zhang, B., Kaur, P., Shimada, H., Groffen, J., Kazimierczuk, Z., Pinna, L. A. and Heisterkamp, N. (2007) Treatment of P190 Bcr/Abl lymphoblastic leukemia cells with inhibitors of the serine/threonine kinase CK2. Leukemia **21**, 178–180
39 Scaglioni, P. P., Yung, T. M., Cai, L. F., Erdjument-Bromage, H., Kaufman, A. J., Singh, B., Teruya-Feldstein, J., Tempst, P. and Pandolfi, P. P. (2006) A CK2-dependent mechanism for degradation of the PML tumor suppressor. Cell **126**, 269–283
40 Ruzzene, M., Penzo, D. and Pinna, L. A. (2002) Protein kinase CK2 inhibitor 4,5,6,7-tetrabromobenzotriazole (TBB) induces apoptosis and caspase-dependent degradation of haematopoietic lineage cell-specific protein 1 (HS1) in Jurkat cells. Biochem. J. **364**, 41–47
41 Druker, B. J. (2005) Clinical aspects of imatinib therapy. In Inhibitors of Protein Kinases and Protein Phosphatases (Pinna, L. A. and Cohen, P. T. W., eds.), pp. 391–411, Springer-Verlag, Berlin, Heidelberg
42 Agullo, G., Gamet-Payrastre, L., Manenti, S., Viala, C., Remesy, C., Chap, H. and Payrastre, B. (1997) Relationship between flavonoid structure and inhibition of phosphatidylinositol 3-kinase: a comparison with tyrosine kinase and protein kinase C inhibition. Biochem. Pharmacol. **53**, 1649–1657
43 Meggio, F., Shugar, D. and Pinna, L. A. (1990) Ribofuranosyl-benzimidazole derivatives as inhibitors of casein kinase-2 and casein kinase-1. Eur. J. Biochem. **187**, 89–94
44 Pagano, M. A., Meggio, F., Ruzzene, M., Andrzejewska, M., Kazimierczuk, Z. and Pinna, L. A. (2004) 2-Dimethylamino-4,5,6,7-tetrabromo-1*H*-benzimidazole: a novel powerful and selective inhibitor of protein kinase CK2. Biochem. Biophys. Res. Commun. **321**, 1040–1044
45 Duncan, J. S., Gyenis, L., Lenehan, J., Bretner, M., Graves, L. M., Haystead, T. A. and Litchfield, D. W. (2008) An unbiased evaluation of CK2 inhibitors by chemo-proteomics: characterization of inhibitor effects on CK2 and identification of novel inhibitor targets. Mol. Cell. Proteomics **7**, 1077–1088
46 Pasqualucci, L., Neumeister, P., Goossens, T., Nanjangud, G., Chaganti, R. S., Kuppers, R. and Dalla Favera, R. (2001) Hypermutation of multiple proto-oncogenes in B-cell diffuse large-cell lymphomas. Nature **412**, 341–346
47 Aikawa, Y., Nguyen, L. A., Isono, K., Takakura, N., Tagata, Y., Schmitz, M. L., Koseki, H. and Kitabayashi, I. (2006) Roles of HIPK1 and HIPK2 in AML1- and p300-dependent transcription, hematopoiesis and blood vessel formation. EMBO J. **25**, 3955–3965
48 Di Stefano, V., Rinaldo, C., Sacchi, A., Soddu, S. and D'Orazi, G. (2004) Homeodomain-interacting protein kinase-2 activity and p53 phosphorylation are critical events for cisplatin-mediated apoptosis. Exp. Cell. Res. **293**, 311–320
49 Manning, G., Whyte, D. B., Martinez, R., Hunter, T. and Sudarsanam, S. (2002) The protein kinase complement of the human genome. Science **298**, 1912–1934

Received 6 February 2008/10 June 2008; accepted 30 June 2008
Published as BJ Immediate Publication 30 June 2008, doi:10.1042/BJ20080309

Biochem. J. (2008) **415**, 353–365 (Printed in Great Britain) doi:10.1042/BJ20080309

online data

SUPPLEMENTARY ONLINE DATA
The selectivity of inhibitors of protein kinase CK2: an update

Mario A. PAGANO*†[1], Jenny BAIN‡[1], Zygmunt KAZIMIERCZUK§[2], Stefania SARNO*†, Maria RUZZENE*†, Giovanni DI MAIRA*†, Matthew ELLIOTT‡, Andrzej ORZESZKO‖, Giorgio COZZA*, Flavio MEGGIO* and Lorenzo A. PINNA*†[1,2]

*Department of Biological Chemistry and CNR Institute of Neurosciences, University of Padova, viale G. Colombo 3, 35121 Padova, Italy, †Venetian Institute for Molecular Medicine (VIMM), via Orus 2, 35129 Padova, Italy, and ‡Division of Signal Transduction Therapy and Medical Research Council, Protein Phosphorylation Unit, University of Dundee, Dundee DD1 5EH, Scotland, U.K., §Laboratory of Experimental Pharmacology, Polish Academy of Sciences Medical Research Center, 5 Pawinskiego St. 02-106 Warsaw, Poland, and ‖Military University of Technology, 2 Kaliskiego Street, 00-908 Warsaw, Poland

EXPERIMENTAL

Details of the synthesis of new compounds

Melting points (uncorrected) were measured in open capillary tubes on a Gallenkamp-5 melting point apparatus. ^{1}H NMR spectra (in p.p.m.) were measured with a model Bruker 400 MHz spectrometer at 298K in D_6DMSO using tetramethylsilane as the internal standard. UV absorption spectra were recorded on a UV8500 spectrophotometer. Mass spectra (70 eV) were obtained with a model AMD-604 Intectra spectrometer. Flash chromatography was performed on silica gel (230–400 mesh; Merck). Elemental analyses of the newly synthesized compounds were within $\pm$0.4 % of the respective theoretical values.

4,5,6,7-Tetrabromo-1*H*-indazole (1, K59)

The suspension of 2-methyl-3,4,5,6-tetrabromoaniline (4 g, 9.5 mmol) in acetic acid anhydride (65 ml) was stirred at 100 °C (bath temperature) for 2 h. The resulting clear solution was cooled to 10 °C and treated with nitrous gases for approx. 6 h (compare with [1]). The almost clear deep blue-green product solution was poured on to a mixture of 200 g of ice and 100 ml of ice-cold water and allowed to stand until the ice melted. The yellow precipitate formed was filtered-off, washed with ice-cold water and kept in a dessicator over solid KOH for 8 h. The dried precipitate was stirred in toluene (100 ml) at room temperature (20 °C) for 2 h and then at 50 °C for 2 days. The resulting pale-yellow solution was evaporated to dryness and the dried residue was purified by dissolving it in ethanol/0.5 M KOH (7:3, approx. 80 ml) solution and precipitating the title compounds from hot solution with acetic acid; the procedure yielded a chromatographically pure white powder (1.9 g, 46 % yield). A sample of the product used for elemental analysis was crystallized from ethanol. Melting point, 290–292 °C [dec. (decomposition)]; ^{1}H NMR (DMSO-d_6) 6.18 (s, C*H*), 14.05 (bs, N*H*); p*K*a (in 50 % EtOH), 10.6; Anal. (analytical data for elemental analysis) ($C_7H_2Br_4N_2$) C, H, N.

1-Hydroxyethyl-4,5,6,7-tetrabromo-1*H*-indazole (2a, K60) and 2-hydroxyethyl-4,5,6,7-tetrabromo-2*H*-indazole (3a, K61)

To the solution of **1** (1 g, 2.375 mmol) in 2-butanone (15 ml) pulverized anhydrous K_2CO_3 (1 g) and 2-bromoethanol (1 g, 8 mmol) were added and the reaction mixture was stirred and refluxed for 6 h. After this period of time the insolubilities were filtered off and the filtrate was evaporated under reduced pressure. Isomers **2a** and **3a** were isolated by flash chromatography using a silica gel column (2 cm $\times$ 50 cm). Chromatography was performed with $CHCl_3$/EtOH (20:3). The faster migrating zone was evaporated to dryness and the residue was crystallized from ethanol/water to give **2a** as colourless crystals (205 mg, 18 %): melting point, 189 °C; ^{1}H NMR (DMSO-d_6) 3.78 (q, CH_2), 4.82 (t, CH_2), 4.86 (t, O*H*), 8.15 (s, C*H*); Anal. ($C_9H_6Br_4N_2O$) C, H, N. The slower migrating zone after evaporation and crystallization from ethanol/water gave crystalline **3a** (295 mg, 26 %): melting point, 192–193 °C; ^{1}H NMR (DMSO-d_6) 3.88 (q, CH_2), 4.51 (t, CH_2), 5.02 (t, O*H*), 8.61 (s, C*H*); Anal. ($C_9H_6Br_4N_2O$) C, H, N.

1-Dimethylaminoethyl-4,5,6,7-tetrabromo-1*H*-indazole (2b, K62) and 2-dimethylaminoethyl-4,5,6,7-tetrabromo-2*H*-indazole (3b, K63)

To the solution of **1** (1 g, 2.375 mmol) in 2-butanone (15 ml) pulverized anhydrous K_2CO_3 (1 g) and hydrochloride of 2-dimethylaminoethyl chloride (1.16 g, 8 mmol) were added and the reaction mixture was stirred and refluxed for 5 h. After this period of time the insolubilities were filtered off and the filtrate was evaporated under reduced pressure. Isomers **2b** and **3b** were isolated by flash chromatography using a silica gel column (2 cm $\times$ 50 cm) and a mixture of chloroform/anhydrous ethanol/ammonia (20:3:0.04) as an eluent. The first migrating zone was evaporated to dryness and the residue was crystallized from ethanol/aqeous ammonia to give colourless crystals of **2a** (250 mg, 21 %): melting point, 92 °C; ^{1}H NMR (DMSO-d_6) 2.18 (s, CH_3), 2.68 (t, CH_2), 4.83 (t, CH_2), 8.15 (s, C*H*); Anal. ($C_{11}H_{11}Br_4N_3$) C, H, N. The slower migrating zone after evaporation and crystallization from ethanol/aqueous ammonia gave crystalline **3b** (205 mg, 17 %): melting point, 139–141 °C; ^{1}H NMR (DMSO-d_6) 2.17 (s, CH_3), 2.79 (t, CH_2), 4.55 (t, CH_2), 8.66 (s, C*H*).

3,4,5,6,7-Pentabromo-1*H*-indazole (4, K64)

4,5,6,7-Tetrabromoindazole (**1**) (150 mg, 0.36 mmol) was dissolved by heating in anhydrous acetic acid (13 ml). The stirred solution was chilled to room temperature and bromine (0.32 ml, 6.25 mmol) was added. The stirring was continued overnight at 90 °C (bath temperature). The reaction mixture was evaporated to dryness and then twice with toluene. The final pale-yellow residue was crystallized from ethanol to give white crystals (135 mg, 72 % yield): melting point, 295–296 °C (dec); ^{1}H NMR (DMSO-d_6) 14.35 (bs, N*H*); p*K*a (in 50 % ethanol), 8.40; Anal. ($C_7HBr_5N_2$) C, H, N.

[1] These authors contributed equally to the present study.
[2] Correspondence may be addressed to either of these authors (email lorenzo.pinna@unipd.it or zygmunt_kazimierczuk@sggw.pl).

Table S1 UV, MS and elemental analysis of newly obtained compounds

Compound	UV λ_{max} (ε_{max}) (MeOH)	MS data (70 eV)	Elemental analysis data
1 (K59)	273.5 (7050), 280 (sh), 306 (5200), 318 (5600)	438 (16), 437 (6), 436 (64), 435 (8), 434 (100), 433 (6), 432 (69), 430 (18)	Analysis calculated for $C_7H_2Br_4N_2$ (433.72): C, 19.38; H, 0.46; N 6.46. Found: C, 19.33; H, 0.54; N, 5.22.
2a (K60)	277 (6200), 316 (5700), 325 (6050)	481 (9), 480 (34), 479 (6), 478 (53), 477 (4), 476 (37), 474 (10), 447 (100)	Analysis calculated for $C_9H_6Br_4N_2O$ (477.78): C 22.63, H 1.27, N 5.86. Found: C 22.48, H 1.35, N 5.67.
3a (K61)	288 (8300), 303 (7800), 318 (7900), 332 (6400)	482 (12), 481 (6), 480 (49), 479 (9), 478 (75), 477 (7), 476 (51), 474 (13), 447 (24) 434 (100)	Analysis calculated for $C_9H_6Br_4N_2O$ (477.78): C 22.63, H 1.27, N 5.86. Found: C 22.52, H 1.36, N 5.75.
2b (K62)	277 (6500), 316 (6000), 325 (6200)	506 (3), 504 (6), 502 (93.5), 475 (8), 460 (12), 447 (58), 58 (100)	Analysis calculated for $C_{11}H_{11}Br_4N_3$ (504.84): C 26.17, H 2.20, N 8.32. Found: C 26.32, H 2.32, N 8.23.
3b (K63)	288 (8600), 303 (8000), 318 (8100), 332 (6600)	506 (4), 504 (7), 502 (5), 465 (18), 447 (49), 434 (96), 58 (100)	Analysis calculated for $C_{11}H_{11}Br_4N_3$ (504.84): C 26.17, H 2.20, N 8.32. Found: C 26.30, H 2.32, N 8.18.
4 (K64)	278 (5700), 289 (4850), 302 (sh), 314 (6500), 326 (7350)	518 (10), 517 (4), 516 (48), 515 (9), 514 (98), 513 (9), 512 (100), 511 (4.6), 510 (51), 508 (11)	Analysis calculated for $C_7HBr_5N_2$ (512.62): C 16.40, H 0.20, N 5.46. Found; C 16.28, H 0.36, N 5.35.
6 (K67)	229 (36 600), 273 (13 700), 312 (5600)	567 (18), 566 (11), 565 (68), 564 (16), 563 (100), 562 (11), 561 (68), 559 (18)	Analysis calculated for $C_{13}H_{13}Br_4N_3O_2$ (562.88): C, 27.74, H, 2.23, N 7.47. Found: C, 27.58, H, 2.34, N, 7.31.
7 (K66)	228 (34 900), 273 (12 600), 312 (7600)	539 (17), 538 (9), 537 (63), 536 (14), 535 (100), 534 (11), 533 (74), 531 (21), 522 (18), 590 (51)	Analysis calculated for $C_{11}H_9Br_4N_3O_2$ (534.83): C, 24.70, H, 1.70, N 7.86. Found: C, 24.68, H, 1.98, N, 7.61.
9 (K72)	258 (31 600), 335 (23 400)	484 (19), 482 (66), 480 (100), 478 (69), 476 (18), 447 (47)	Analysis calculated for $C_8H_4Br_4N_2S$ (479.81): C, 20.03, H, 0.84, N, 5.84. Found: C, 20.24, H, 1.02, N, 5.73.
10	238 (32 300), 278 (12 200), 301 (9300), 313 (11 300)	569 (6), 567 (21), 565 (33), 563 (23), 561 (5), 493 (100)	Analysis calculated for $C_{12}H_{10}Br_4N_2O_2S$ (565.91): C, 25.47, H, 1.78, N, 4.95. Found: C, 25.44, H, 1.82, N, 4.79.
11 (K74)	238 (34 400), 278 (11 800), 301 (9900), 313 (14 600)	554 (10), 552 (37), 550 (49), 548 (35), 546 (9), 493 (100)	Analysis calculated for $C_{11}H_9Br_4N_3OS$ (550.89): C, 23.98, H, 1.65, N, 7.63. Found: C, 23.85, H, 1.77, N, 7.44.
12 (K75)	236 (34 400), 279 (12 200), 301 (9200), 313 (11 300)	541 (7), 539 (25), 537 (35), 535 (25), 533 (7), 493 (65), 463 (100)	Analysis calculated for $C_{10}H_6Br_4N_2O_2S$ (537.85): C, 22.33, H, 1.12, N, 5.21. Found: C, 22.44, H, 1.25, N, 5.02.

Table S2 Profiling a library of compounds on CK2, PIM1 and HIPK2

The residual activity of CK2, PIM1 and HIPK2 at an inhibitor concentration of 20 μM is shown. Phosphorylation conditions are described in the Experimental section of the main text at the indicated concentration of ATP. Residual activity was determined as detailed in the legend of Table 1 of the main text. Residual activities $\leqslant$15 % are shown in bold.

Derivative

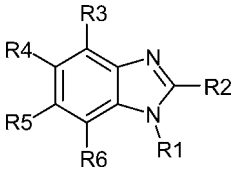

	R1	R2	R3	R4	R5	R6	Reference*	CK2	PIM1	HIPK2
K1	H	CF_3	H	H	H	H	[2]	98.5	76.1	80.1
K4	H	CF_3	H	Br	H	H	[2]	87.8	81.2	78.0
K5	H	CF_3	H	Br	Br	H	[2]	58.6	56.1	60.6
K6	H	CF_3	Br	H	Br	H	[2]	79.2	74.7	90.5
K7	H	CF_3	Br	Br	Br	H	[2]	**12.5**	17.6	37.4
K8	H	C_2F_5	Br	H	Br	H	[3]	41.8	50.9	60.8
K9	H	$SCH_2CH_2N(CH_3)_2$	Br	H	Br	H	[3]	88.0	81.2	93.8
K10	H	CF_3	Br	Br	Br	Br	[2]	**8.3**	**10.3**	32.0
K11	H	C_2F_5	Br	Br	Br	Br	[3]	**5.1**	**8.6**	n.d.
K15	C_2H_5	CF_3	Br	Br	Br	Br	[4]	37.7	60.1	49.5
K16	H	CF_3	Br	Cl	Cl	Br	[4]	**11.4**	**12.0**	45.2
K17 (TBI)	H	H	Br	Br	Br	Br	[4]	**6.0**	**8.2**	**13.4**
K18	H	CF_3	Br	Cl	Br	Cl	[4]	**10.6**	**10.1**	25.7
K19	H	CF_3	Br	Cl	Br	Br	[4]	**4.5**	**8.2**	46.9
K20	H	Br	Br	Br	Br	Br	[4]	**7.1**	**10.6**	20.7
K21	H	Cl	Br	Br	Br	Br	[4]	**5.1**	**9.9**	25.4
K22	H	=S	Br	Br	Br	Br	[4]	**5.8**	**11.6**	19.1
K24	H	$NHCH_3$	Br	Br	Br	Br	[5]	**5.7**	**3.4**	n.d.
K25 (DMAT)	H	$N(CH_3)_2$	Br	Br	Br	Br	[5]	**6.1**	**5.1**	**8.3**
K26	H	$NHCH_2CHOHCH_3$	Br	Br	Br	Br	[5]	**8.3**	**2.0**	**12.5**
K27	H	NH_2	Br	Br	Br	Br	[5]	**5.0**	**4.5**	16.0
K28	CH_3	=O	Br	Br	Br	Br	[5]	**11.1**	83.9	**9.3**
K29	H	$NHCH(CH_3)_2$	Br	Br	Br	Br	[5]	**4.2**	**5.7**	76.4
K30	H	$NHCH_2CH_2OH$	Br	Br	Br	Br	[5]	**5.5**	**5.8**	24.6
K31	H	$NHCH_2CH_2N(CH_3)_2$	Br	Br	Br	Br	[5]	**4.8**	**3.6**	**8.8**
K32	H	=O	Br	Br	Br	Br	[5]	15.9	78.7	**6.9**
K33	H	SCH_2COOH	Br	Br	Br	Br	[5]	**6.2**	15.2	73.0
K34	H	$SCH_2(C_6H_4)NO_2$	Br	Br	Br	Br	[5]	38.4	93.4	n.d.
K35	H	$SCH_2COOC_2H_5$	Br	Br	Br	Br	[5]	18.6	**13.0**	n.d.
K36	CH_3	SCH_3	Br	Br	Br	Br	[5]	**13.0**	90.1	34.6
K38	CH_3	OC_2H_5	Br	Br	Br	Br	[5]	58.9	82.5	84.7
K39	CH_3	$OCH(CH_3)_2$	Br	Br	Br	Br	[5]	49.1	43.0	88.7
K40	CH_3	$N(CH_3)_2$	Br	Br	Br	Br	[5]	**6.4**	19.7	24.7
K41	CH_3	$NHCH(CH_3)_2$	Br	Br	Br	Br	[5]	**7.5**	**10.5**	25.1
K42	H	$SCH_2CH(OH)CH_2OH$	Br	Br	Br	Br	[5]	**3.7**	**4.2**	19.0
K43	CH_3	H	Br	Br	Br	Br	[6]	**12.1**	21.0	31.4
K44	C^2-$N(CH_3)CH_2CH_2$-N^1		Br	Br	Br	Br	[7]	**10.0**	**11.5**	21.4
K45	CH_2CHCH_2	Br	Br	Br	Br	Br	[5]	20.3	59.8	25.1
K46	$CH_2C(O)NH_2$	Br	Br	Br	Br	Br	[5]	27.2	n.d.	n.d.
K49	H	$N(CH_3)CH_2CH_2OH$	Br	Br	Br	Br	[7]	**3.7**	**4.3**	**11.1**
K50	C^2-$NHCH_2CH_2CH_2$-N^1		Br	Br	Br	Br	K. Zawada, M. Wolniak, Z. Kazimierczuk and I. Wawer, unpublished work	49.8	68.7	83.0
K51	C^2-$NHCH_2CH_2$-N^1		Br	Br	Br	Br	K. Zawada, M. Wolniak, Z. Kazimierczuk and I. Wawer, unpublished work	47.3	46.6	57.0
K52	H	$NHCH_2CH_2CH_2OH$	Br	Br	Br	Br	K. Zawada, M. Wolniak, Z. Kazimierczuk and I. Wawer, unpublished work	**4.4**	**2.3**	**11.3**
K53	H	SCH_2CH_2OH	Br	Br	Br	Br	K. Zawada, M. Wolniak, Z. Kazimierczuk and I. Wawer, unpublished work	**5.1**	**5.9**	**12.9**
K54	C^2-SCH_2CH_2-N^1		Br	Br	Br	Br	K. Zawada, M. Wolniak, Z. Kazimierczuk and I. Wawer, unpublished work	26.7	46.6	32.1
K55	C^2-$SCH_2CH_2CH_2$-N^1		Br	Br	Br	Br	K. Zawada, M. Wolniak, Z. Kazimierczuk and I. Wawer, unpublished work	**12.0**	32.9	27.4
K56	H	$SCH_2CH_2CH_2OH$	Br	Br	Br	Br	K. Zawada, M. Wolniak, Z. Kazimierczuk and I. Wawer, unpublished work	**3.3**	**3.9**	15.5
K59 (**1**)	-	-	-	-	-	-	The present study	**6.4**	40.0	51.0
K60 (**2a**)	-	-	-	-	-	-	The present study	**12.4**	43.7	64.9
K61 (**3a**)	-	-	-	-	-	-	The present study	**8.2**	18.1	32.6
K62 (**2b**)	-	-	-	-	-	-	The present study	**8.5**	22.3	61.7
K63 (**3b**)	-	-	-	-	-	-	The present study	**9.1**	**9.5**	41.6
K64 (**4**)	-	-	-	-	-	-	The present study	**5.4**	26.6	36.1

Table S2—(*Contd*.)

K66 (**7**)	CH_2COOH	$N(CH_3)_2$	Br	Br	Br	Br	The present study	**9.0**	72.0	70.8
K67 (**6**)	$CH_2COC_2H_5$	$N(CH_3)_2$	Br	Br	Br	Br	The present study	**11.2**	27.8	81.4
K68	CH_2COOH	H	Br	Br	Br	Br	K. Zawada, M. Wolniak, Z. Kazimierczuk and I. Wawer, unpublished work	23.5	89.2	86.9
K69	$CH_2COC_2H_5$	H	Br	Br	Br	Br	K. Zawada, M. Wolniak, Z. Kazimierczuk and I. Wawer, unpublished work	32.8	47.5	66.1
K72 (**9**)	CH_3	=S	Br	Br	Br	Br	The present study	**4.6**	22.9	70.0
K73	CH_3	SCH_2CONH_2	Br	Br	Br	Br	K. Zawada, M. Wolniak, Z. Kazimierczuk and I. Wawer, unpublished work	**5.1**	18.5	75.4
K74 (**11**)	CH_3	$SCH_2CONHCH_3$	Br	Br	Br	Br	The present study	**12.6**	76.2	95.7
K75 (**12**)	CH_3	SCH_2COOH	Br	Br	Br	Br	The present study	**8.4**	40.9	64.9
K83	CH_2CONH_2	H	Br	Br	Br	Br	K. Zawada, M. Wolniak, Z. Kazimierczuk and I. Wawer, unpublished work	17.5	79.0	87.5
K84	$CH_2CONHCH_3$	H	Br	Br	Br	Br	K. Zawada, M. Wolniak, Z. Kazimierczuk and I. Wawer, unpublished work	51.0	66.1	69.2
K85	$CH_2CONHNH_2$	H	Br	Br	Br	Br	K. Zawada, M. Wolniak, Z. Kazimierczuk and I. Wawer, unpublished work	32.3	48.7	73.1
K86	CH_3	$SCH_2CONHNH_2$	Br	Br	Br	Br	K. Zawada, M. Wolniak, Z. Kazimierczuk and I. Wawer, unpublished work	**13.7**	53.1	58.4
K87	CH_3	$NHNH_2$	Br	Br	Br	Br	K. Zawada, M. Wolniak, Z. Kazimierczuk and I. Wawer, unpublished work	**7.2**	23.6	32.7
K90	CH_3	SCH_2CH_2OH	Br	Br	Br	Br	K. Zawada, M. Wolniak, Z. Kazimierczuk and I. Wawer, unpublished work	**8.6**	28.4	47.2
K91	CH_3	$SCH_2CH_2CH_2OH$	Br	Br	Br	Br	K. Zawada, M. Wolniak, Z. Kazimierczuk and I. Wawer, unpublished work	15.9	27.8	60.0

*Reference with a detailed description of the synthesis of the compound.

(2-Dimethylamino-4,5,6,7-tetrabromobenzoimidazol-1-yl)-acetic acid ethyl ester (6, K67)

The mixture of 2-dimethylamino-4,5,6,7-tetrabromobenzimidazole (**5**) (540 mg, 1.15 mmol), K_2CO_3 (1 g), bromoacetic acid ethyl ester (400 mg, 2.4 mmol) in 45 ml acetone was stirred at 60 °C (bath temperature) for 10 h. The insolubilities were filtered off and washed with 50 ml of hot acetone. The filtrate and washing were combined and evaporated to dryness. The residue was crystallized from ethanol to give white needles (520 mg, 80 %). ^{1}H NMR (DMSO-d_6), 1.22 (t, CH_3), 2.95 (s, $2 \times CH_3$), 4.20 (q, CH_2), 5.04 (s, CH_2); Anal. ($C_{13}H_{13}Br_4N_3O_2$) C, H, N.

(2-Dimethylamino-4,5,6,7-tetrabromobenzoimidazol-1-yl)-acetic acid (7, K66)

The suspension of **6** (520 mg, 1 mmol) in solution of KOH (280 mg, 5 mmol) in ethanol/water [3:1 (v/v), 16 ml] was stirred at room temperature for 3 h. After 2 h the mixture became clear. The solution was brought to pH 2–3 with concentrated HCl. The white chromatographically pure precipitate was filtered and washed with water (390 mg, 73 %). A sample for analysis was crystallized from dioxane: melting point, 284–287 °C (dec.); ^{1}H NMR (DMSO-d_6), 2.95 (s, $2 \times CH_3$), 4.96 (s, CH_2), 13.5 (bs, OH); Anal. ($C_{11}H_9Br_4N_3O_2$) C, H, N.

4,5,6,7-Tetrabromo-methyl-1,3-dihydro-benzimidazole-2-thione (9, K72)

The mixture of **8** (530 mg, 1 mmol) and thiourea (460 mg, 6 mmol) in propan-1-ol (60 ml) was stirred and refluxed for 12 h. Next, it was chilled and the formed precipitate was filtered off and washed with a small volume of water and ethanol (460 mg, 96 %). The chromatographically pure material was used for the further steps without crystallization. A sample for analysis and biological investigations was crystallized from methoxyethanol. Melting point, 310–312 °C [with dec. (subtance decomposes during melting)]; ^{1}H NMR (DMSO-d_6), 3.99 (s, CH_3), 13.56 (s, HN); Anal. ($C_8H_4Br_4N_2S$) C, H, N.

(4,5,6,7-Tetrabromo-1-methyl-1H-benzoimidazol-2-ylsulfanyl)-acetic acid ethyl ester (10)

To the stirred mixture of **9** (720 mg, 1.5 mmol), finely pulverized anhydrous K_2CO_3 (1.5 g) in acetone (75 ml) and bromoacetic acid ethyl ester (830 mg, 5 mmol) was added. The mixture was stirred and refluxed for 3 h. The insolubilities were filtered off and the filtrate cake was washed with warm acetone (50 ml). The filtrate and washings were combined, evaporated to dryness and the residue was crystallized from ethanol to give colourless needles (650 mg, 77 %). Melting point, 127–128 °C; ^{1}H NMR (DMSO-d_6), 1.21 (t, CH_3), 3.95 (s, N-CH_3), 4.15 (q, CH_2), 4.28 (s, SCH_2); Anal. ($C_{12}H_{10}Br_4N_2O_2S$) C, H, N.

(4,5,6,7-Tetrabromo-1-methyl-1H-benzoimidazol-2-ylsulfanyl)-acetic acid (12, K75)

To the solution of **10** (395 mg, 0.7 mmol) in ethanolic KOH (25 ml ethanol, 340 mg KOH, 6 mmol) bromoacetic acid (230 mg, 1.5 mmol) was added. The mixture was stirred at room temperature for 24 h. Then it was brought to pH 2–3 with 1 M HCl. The precipitate was filtered and crystallized from dioxane/water to give white powder (330 mg, 88 %). Melting point, 205–207 °C (dec.); ^{1}H NMR (DMSO-d_6), 3.95 (s, CH_3), 4.25 (s, CH_2), 13.05 (bs, OH); Anal. ($C_{10}H_6Br_4N_2O_2S$) C, H, N.

N-Methyl-2-(4,5,6,7-tetrabromo-1-methyl-1H-benzoimidazol-2-ylsulfanyl)-acetamide (11, K74)

The suspension of **10** (280 mg, 0.5 mmol) in ethanolic methylamine (25 ml, 20 %) was stirred at room temperature for 2 days.

The precipitate was filtered off and crystallized from dioxane to give a white cotton-like product (235 mg, 85 %). Melting point, 252–254 °C (with dec.); ^{1}H NMR, 2.63 (d, N-CH_3), 3.93 (s, CH_3), 4.14 (s, CH_2), 8.29 (bs, NH); Anal. ($C_{11}H_9Br_4N_3OS$) C, H, N.

REFERENCES

1 Organic Syntheses, Coll. Vol. 5, p 650 (1973)
2 Büchel, K. H. (1970) Herbizide Trifluoromethyl-benzimidazole Z. Naturforsch **25b**, 934–944
3 Andrzejewska, M., Yepez-Mulia, L., Cedillo-Rivera, R., Tapia, A., Vilpo, L., Vilpo, J. and Kazimierczuk, Z. (2002) Synthesis, antiprotozoal and anticancer activity of substituted 2-trifluoromethyl- and 2-pentafluoroethylbenzimidazoles. Eur. J. Med. Chem. **37**, 973–978
4 Andrzejewska, M., Pagano, M. A., Meggio, F., Brunati, M. and Kazimierczuk, Z. (2003) Polyhalogenobenzimidazoles: synthesis and their inhibitory activity against casein kinases. Bioorg. Med. Chem. **11**, 3997–4002
5 Pagano, M. A., Andrzejewska, M., Ruzzene, M., Sarno, S., Cesaro, L., Bain, J., Elliott, M., Meggio, F., Kazimierczuk, Z. and Pinna, LA. (2004) Optimization of protein kinase CK2 inhibitors derived from 4,5,6,7-tetrabromobenzimidazole. J. Med. Chem. **47**, 6239–6247
6 Kopanska, K., Najda, A., Zebrowska, J., Chomicz, L., Piekarczyk, J., Myjak, P. and Bretner, M. (2004) Synthesis and activity of 1H-benzimidazole and 1H-benzotriazole derivatives as inhibitors of *Acanthamoeba castellanii*. Bioorg. Med. Chem. **12**, 2617–2624
7 Battistutta, R., Mazzorana, M., Sarno, S., Kazimierczuk, Z., Zanotti, G. and Pinna, L. A. (2005) Inspecting the structure–activity relationship of protein kinase CK2 inhibitors derived from tetrabromo-benzimidazole. Chem. Biol. **12**, 1211–1219

Received 6 February 2008/10 June 2008; accepted 30 June 2008
Published as BJ Immediate Publication 30 June 2008, doi:10.1042/BJ20080309